

# Data-driven model selection within the matrix completion method for causal panel data models.

Sandro Heiniger<sup>1</sup>

<sup>1</sup>University of St.Gallen, sandro.heiniger@unisg.ch

## Abstract

Matrix completion estimators are employed in causal panel data models to regulate the rank of the underlying factor model using nuclear norm minimization. This convex optimization problem enables concurrent regularization of a potentially high-dimensional set of covariates to shrink the model size. For valid finite sample inference, we adopt a permutation-based approach and prove its validity for any treatment assignment mechanism. Simulations illustrate the consistency of the proposed estimator in parameter estimation and variable selection. An application to public health policies in Germany demonstrates the data-driven model selection feature on empirical data and finds no effect of travel restrictions on the containment of severe Covid-19 infections.

*Matrix completion; Model selection; Panel data; Regularisation;*

## 1 Introduction

The prevalence of big data and high-dimensional covariate spaces has grown significantly in applied economics (see Jin et al. [2015] for an overview). Consequently, the econometric literature strives to develop suitable tools to cater to the needs of applied research (e.g., Belloni et al. [2014], Farrell [2015], Belloni et al. [2017], Ning et al. [2020]). One widely employed framework in this context is the  $l_1$  regularization, known as *lasso*, which facilitates model selection and feature extraction by regulating covariate parameters. Fan and Li [2006]

provide an extensive discussion on the pivotal role of model selection for knowledge discovery and addressing high-dimensionality challenges.

Rigorous sparse model selection methods offer key advantages in terms of prediction accuracy and interpretability [Tibshirani, 1996]. Beyond prediction tasks, lasso techniques have found substantial utility in causal analysis. Even though for causal identification strategies that rely on the unconfoundedness assumption [Rosenbaum and Rubin, 1983], the role of covariates narrows down to including all confounding variables in the data, model selection nevertheless offers significant features:

- 1) Common estimators often rely on estimating an outcome/propensity score model to evaluate unobserved potential outcomes or as a nuisance function. Precise estimation of those underlying models can lead to significant gains in prediction accuracy for causal estimands in finite samples.

- 2) In the absence of theoretical guidance on the true model, researchers may face a high-dimensional problem, where the number of parameters exceeds available observations (often referred to as ' $p \gg n$ ' or 'The Curse of Dimensionality'). In such scenarios, estimators like the linear regression family are inapplicable due to insufficient degrees of freedom, necessitating dimensionality reduction.

- 3) The econometric literature has proposed various variants of post-regularization estimation methods [Chernozhukov et al., 2015]. If the initial model selection step achieves sufficient sparsity, a second non-regularized estimation of the resulting parsimonious model may even become the oracle estimator when the true model is identified [Belloni and Chernozhukov, 2013].

- 4) Recent years have witnessed a significant surge in interest in estimating and analyzing heterogeneous treatment effects [Künzel et al., 2019]. A model selection feature can offer valuable support and guidance for selecting potential heterogeneity dimensions.

All the aforementioned points are strongly supported by the prevalence of low-rank matrices in high-dimensional data, as demonstrated in Udell and Townsend [2019]. It has been

shown that *lasso* can consistently identify such sparse models while achieving convergence at the optimal rate concerning the parameters of interest (known as the *oracle property*) under specific conditions [Meinshausen and Bühlmann, 2006, Zou, 2006, Meinshausen, 2007].

Our main contribution lies in extending the use of  $l_1$  regularization to matrix completion estimators for causal panel data models. In their seminal work, Athey et al. [2021] lay the foundation for employing matrix completion methods in causal panel data models. This estimator utilizes observed elements of control outcomes to impute the unobserved (*missing*) potential outcomes of treated observations in the untreated state. By interpreting the panel data structure as a matrix, this procedure approximates the complete matrix of control state potential outcomes by regularizing the complexity of the underlying factor model using the nuclear norm. Matrix completion estimation has been shown to outperform synthetic control estimators or regression methods based on the unconfoundedness assumption [Athey et al., 2019, 2021], and its initial applications have shown its practical value [Wood et al., 2020, Rafaty et al., 2020, Levy and Mattsson, 2022]. Appendix A provides background of the matrix completion estimator and an embedding in the context of causal panel data models.

In this work, we leverage the convex nature of nuclear norm minimization to regularize the rank of the general factor matrix. In a model with covariates, this allows for concurrent regularization of a potentially high-dimensional set of variables. Unlike other estimation methods, where  $l_1$  regularization often increases the numerical complexity of an estimator by lacking a closed-form solution, preserves  $l_1$  regularization of covariate parameters the convex optimization of rank regularization in matrix completion estimators, thus adding no additional complexity. The addition of  $l_1$  regularization to the covariate space enhances the matrix completion framework with a model selection property, thus enhancing its performance in the context of causal panel data analysis without increasing the computational complexity. The methodology allows for a two-step approach similar to common post-regularisation estimators: Involving the selection of the optimal model as the first step and conducting a second estimation without covariate regularization ensuring unbiased estimates of model

parameters.

We adopt the permutation-based inference procedure presented in Chernozhukov et al. [2021] to test the sharp null hypothesis of a zero treatment effect, accommodating a stationary and weakly dependent shock process. The validity of this inference procedure is established not only for the proposed estimator with integrated  $l_1$  covariate regularization but also, as a second contribution, for settings with any treatment assignment scheme. This contribution extends the set of potential applications of matrix completion methods with integrated model selection properties by enabling their use in diverse settings with various treatment assignment mechanisms. This advancement enhances the robustness and versatility of our proposed approach, making it well-suited for a wide range of real-world scenarios.

A numerical simulation using the proposed estimator demonstrates that the introduced  $l_1$  regularization on the covariate space within the matrix completion estimator effectively reduces the determined model size, as intended. Employing a cross-validation step to determine the optimal penalty parameter value justifies adopting a  $1se$  optimality criterion to obtain the ideal model size. The resulting model sizes using the  $1se$  condition are shown to be precise and appear to converge to the true values of the underlying model for large sample sizes.

The proposed estimator outperforms the matrix completion estimator without covariate regularization, in particular for small sample sizes or strong signal-to-noise ratios, and it remains equally precise in other settings. The permutation-based approach necessitates enforcing the null hypothesis for exact and valid inference. However, this requirement may lead to a biased treatment effect estimation if the null hypothesis does not hold. In Section 2, we shed light on how this impacts the estimation procedure and identify the conditions under which a simple rule-of-thumb correction of the treatment effect estimate can be applied. The simulation results reveal that this correction partially mitigates the downward bias and achieves equal estimation accuracy as the unbiased estimates when discarding

the null hypothesis required for inference. Executing a two-stage approach with a second non-regularized estimation on the initially determined model does not yield an improved estimation of the treatment effect on the treated.

An illustrative application examining the impact of travel restriction policies implemented during the Covid-19 pandemic on the incidence of infections requiring treatment in intensive care units underscores the advantageous properties of the model selection mechanism. Within a high-dimensional context characterized by a presumed minuscule signal-to-noise ratio, the proposed estimator adeptly identifies a notably sparse model. The empirical application using panel data aligns precisely with the anticipated behavior of the estimator, as derived from the simulation study. The findings reveal that the estimated effect of the mandatory testing requirement upon entry from foreign countries with heightened incidence rates is small coming along with a notably large p-value. This compelling evidence suggests that the influence of this particular travel restriction policy on public health outcomes is negligible.

To facilitate the adoption and replication of our methodology, we have developed an R-package that implements our proposed estimator. The package is publicly available for download on our GitHub repository.<sup>1</sup> We encourage researchers to utilize our methodology, validate our findings, and contribute to advancements in the field.

The remainder of the article reads as follows: In Section 2, we explain how the model selection property is incorporated into the estimator. Section 3 discusses the theoretical properties of the proposed estimator. The behavior of the proposed estimator in simulations is presented in Section 4. Section 5 discusses the results of the illustrative application to Covid-19 infections in Germany. Finally, we conclude in Section 6. In the Appendix, we provide an introduction to the matrix completion estimator for causal panel data models, additional estimation results and proofs for the theoretical findings.

---

<sup>1</sup>[github.com/heinigersandro/MC\\_MS](https://github.com/heinigersandro/MC_MS)

## 2 Data-driven model selection within matrix completion estimators

We consider a panel of  $N$  units observed over  $T$  periods, where each unit  $i$  potentially undergoes a binary treatment in time-period  $t$ ,  $W_{it} \in \{0, 1\}$ , with corresponding potential outcomes  $Y_{it}(0) := Y_{it}(W_{it} = 0)$  and  $Y_{it}(1) := Y_{it}(W_{it} = 1)$ . Our object of interest is the average treatment effect on the treated<sup>2</sup>, defined as follows:

$$\tau_{\text{ATET}} = \mathbb{E}_{(i,t):W_{it}=1} [Y_{it}(1) - Y_{it}(0)]. \quad (1)$$

We leverage the model with covariates proposed in Athey et al. [2021]:

$$\mathbf{Y} = \mathbf{\Theta} \circ \mathbf{W} + \mathbf{L}^* + \mathbf{X}\mathbf{H}^*\mathbf{Z} + [\mathbf{V}_{it}^\top \boldsymbol{\beta}^*]_{it} + \mathbf{\Gamma}^* \mathbf{1}_T^\top + \mathbf{1}_N (\boldsymbol{\Delta}^*)^\top + \mathbf{U}, \quad (2)$$

where  $\mathbf{Y} \in \mathbb{R}^{N \times T}$  represents the realized outcomes,  $\mathbf{\Theta} \in \mathbb{R}^{N \times T}$  is the matrix of potentially heterogeneous treatment effects,  $\mathbf{W} \in \mathbb{R}^{N \times T}$  denotes the treatment allocation,  $\mathbf{L}^* \in \mathbb{R}^{N \times T}$  represents the unobserved factor matrix of low-rank,  $\mathbf{X} \in \mathbb{R}^{N \times P}$  contains unit-specific covariates,  $\mathbf{Z} \in \mathbb{R}^{Q \times T}$  contains time-specific covariates,  $\mathbf{V}_{it} \in \mathbb{R}^J$  contains the unit-time varying covariates for unit  $i$  at time  $t$ ,  $\mathbf{H}^* \in \mathbb{R}^{P \times Q}$  and  $\boldsymbol{\beta}^* \in \mathbb{R}^J$  are the unknown covariate parameters,  $\mathbf{\Gamma} \in \mathbb{R}^N$  represents unit-level fixed effects,  $\boldsymbol{\Delta} \in \mathbb{R}^T$  represents time-level fixed effects, and  $\mathbf{U} \in \mathbb{R}^{N \times T}$  is a random shock term.

**Assumption 1** (Identifying conditions). *Assume that  $E[\mathbf{U} \mid \mathbf{L}, \mathbf{H}, \boldsymbol{\beta}, \mathbf{\Gamma}, \boldsymbol{\Delta}] = 0$ , and that  $\forall_{i \neq j} : \mathbf{U}_{i,\cdot} \perp\!\!\!\perp \mathbf{U}_{j,\cdot} \mid \mathbf{L}, \mathbf{H}, \boldsymbol{\beta}, \mathbf{\Gamma}, \boldsymbol{\Delta}$ .*

**Assumption 2** (Regularity of stochastic shock). *Suppose that the observed outcomes follow the model (2). Assume that for each observation  $i$ , the stochastic process  $\{\mathbf{U}_{it}\}_{t=1}^T$  satisfies one of the following conditions:*

1.  $\{\mathbf{U}_{it}\}_{t=1}^T$  are iid, or
2.  $\{\mathbf{U}_{it}\}_{t=1}^T$  are stationary, strongly mixing, with sum of mixing coefficients bounded by  $M$ .

---

<sup>2</sup>As reasoned in Appendix A, we assume most observations to be in the untreated state and therefore restrict the focus on the ATET.

Following the literature on factor models, we use an additive and linear model in (2). Despite appearing restrictive, the set of covariates is not limited in size, allowing for the inclusion of any functional forms if desired. More complex interactive terms are absorbed by the latent matrix  $\mathbf{L}^*$  and potentially by the fixed effects as well, granting the model (2) sufficient flexibility to cover a broad range of applications.

The structure of  $\mathbf{H}$  in the outcome model (2) allows only for linked unit- and time-covariate effects. To include linear terms in both  $\mathbf{X}$  and  $\mathbf{Z}$ , a more comprehensive model can be defined as follows:

$$\mathbf{Y} = \boldsymbol{\Theta} \circ \mathbf{W} + \mathbf{L}^* + \tilde{\mathbf{X}}\tilde{\mathbf{H}}^*\tilde{\mathbf{Z}} + [\mathbf{V}_{it}^\top \boldsymbol{\beta}^*]_{it} + \boldsymbol{\Gamma}^* \mathbf{1}_T^\top + \mathbf{1}_N(\boldsymbol{\Delta}^*)^\top + \mathbf{U}, \quad (3)$$

where  $\tilde{\mathbf{X}} = [\mathbf{X} | \mathbf{I}_{N \times N}]$  and  $\tilde{\mathbf{Z}} = [\mathbf{Z}^\top | \mathbf{I}_{T \times T}]^\top$ . For brevity, we focus on the covariate setting as in (2) since all adaptations to the richer model (3) are straightforward.

We define the set of treated observations as  $\mathcal{M} := \{(i, t) \text{ with } W_{it} = 1\}$  and the set of control observations as  $\mathcal{O} := \{(i, t) \text{ with } W_{it} = 0\}$ . Correspondingly, we define the matrices projecting on the respective treatment allocation space as follows:

$$\mathbf{P}_{\mathcal{O}}(A)_{it} = \begin{cases} \mathbf{A}_{it} & \text{if } (i, t) \in \mathcal{O} \\ 0 & \text{if } (i, t) \notin \mathcal{O} \end{cases}$$

$$\mathbf{P}_{\mathcal{M}}(A)_{it} = \begin{cases} \mathbf{A}_{it} & \text{if } (i, t) \in \mathcal{M} \\ 0 & \text{if } (i, t) \notin \mathcal{M} \end{cases}.$$

Using the defined notation and supposing Assumption 1 holds, we can rewrite the sample representation of the ATET, which is our object of interest, as follows:

$$\hat{\tau}_{\text{ATET}} = \frac{1}{|\mathcal{M}|} \sum_{(i,t) \in \mathcal{M}} \mathbf{P}_{\mathcal{M}}(\mathbf{Y} - \hat{\mathbf{Y}}(0)). \quad (4)$$

To evaluate the estimator (4), we only need the matrix of potential outcomes in the absence of treatment, denoted by  $\mathbf{Y}(0)$ . As for each observation, only one potential outcome is realized, some elements in  $\mathbf{Y}(0)$  are missing as they are not observed in practice. The outcome model (2) directly defines the potential outcome model as follows:

$$\mathbf{Y}(0) = \mathbf{L}^* + \mathbf{X}\mathbf{H}^*\mathbf{Z} + [\mathbf{V}_{it}^\top \boldsymbol{\beta}^*]_{it} + \boldsymbol{\Gamma}^* \mathbf{1}_T^\top + \mathbf{1}_N(\boldsymbol{\Delta}^*)^\top + \mathbf{U}. \quad (5)$$

We estimate the unknown parameters of the potential outcome model (5) using a matrix completion method similar to Athey et al. [2021] and Chernozhukov et al. [2021], but with regularization on the full covariate space<sup>34</sup>. We adopt the permutation-based procedure for valid finite sample inference described in Chernozhukov et al. [2021]. The method requires the enforcement of the null hypothesis of a zero treatment effect to obtain a valid and exact inference procedure.<sup>5</sup> In fact, Chernozhukov et al. [2021] show that the rejection rates are substantially erroneous if the null is not enforced. The presumed absence of a treatment effect implies that there is no missing data, which is conterminous to estimating the model parameters using all observations in the panel. This fundamentally differentiates the Chernozhukov et al. [2021] estimation approach from Athey et al. [2021] which guarantees finite sample bounds for the effect estimates but no valid inference.

The estimation procedure is as follows:

$$(\hat{\mathbf{L}}, \hat{\mathbf{H}}, \hat{\boldsymbol{\beta}}, \hat{\boldsymbol{\Gamma}}, \hat{\boldsymbol{\Delta}}) = \arg \min_{\mathbf{L}, \mathbf{H}, \boldsymbol{\beta}, \boldsymbol{\Gamma}, \boldsymbol{\Delta}} \left\{ \frac{1}{NT} \left\| \mathbf{Y} - \mathbf{L} - \mathbf{X}\mathbf{H}\mathbf{Z} - [\mathbf{V}_{it}^\top \boldsymbol{\beta}]_{it} - \boldsymbol{\Gamma} \mathbf{1}_T^\top - \mathbf{1}_N (\boldsymbol{\Delta})^\top \right\|_F^2 + \lambda_L \|\mathbf{L}\|_* + \lambda_H \|\mathbf{H}\|_{1,e} + \lambda_\beta \|\boldsymbol{\beta}\|_{1,e} \right\}, \quad (6)$$

where  $\|\mathbf{A}\|_F^2 = \sum_{(i,t)} \mathbf{A}_{it}^2$  is the squared Fröbenius norm,  $\|\mathbf{A}\|_* = \sum_{i=1}^N \sigma_i(\mathbf{A})$  is the nuclear norm, and  $\|\mathbf{A}\|_{1,e} = \sum_{(i,t)} |\mathbf{A}_{it}|$  is the element-wise  $l_1$  norm.

The choice of the nuclear norm on  $\mathbf{L}$  is crucial as it regularizes the rank of the matrix through its singular values  $\sigma_i(\mathbf{L})$ . Using other norms, such as the Frobenius or element-wise  $l_1$  norm, would not be suitable, as the objective function would be minimized by setting  $\mathbf{L}_{it} = 0$  for all  $(i, t) \in \mathcal{M}$  due to the projection on the control space  $\mathbf{P}_\mathcal{O}$ . The rank norm  $\|\mathbf{A}\|_0 = \sum_{i=1}^N \mathbf{1}\{\sigma_i(\mathbf{L}) > 0\}$ , which might be a preferred choice, is computationally infeasible

---

<sup>3</sup>In Athey et al. [2021], the model with covariates drafts a penalty term on the link matrix  $\mathbf{H}$  between unit- and time-varying covariates, but not on the unit-time-varying covariate parameters  $\boldsymbol{\beta}$ . Though, the authors do not discuss the implications of covariate space regularization on the model selection properties of the proposed estimator.

<sup>4</sup>In principle, the unit- and time-level fixed effects could be regularized as well. We follow the arguments of Hastie et al. [2009] that regularizing the intercept in  $l_1$  regularization increases the bias (see also the discussion in Athey et al. [2021]).

<sup>5</sup>The intuition for this is that the permutation-based inference requires the estimation to be provably accurate across the whole unit-time space to obtain equally distributed residuals. Enforcing the null allows us to use all information in the data, regardless of the treatment state.



as the rank norm optimization is NP-hard [Recht et al., 2010]. On the other hand, the choice of the other norms is straightforward. The Frobenius norm on the prediction error represents an MSE-like measure, while the  $l_1$  regularization on the covariate parameters facilitates the model selection process.

The proposed estimator (6) can be efficiently computed by iteratively applying a *soft-impute* step [Mazumder et al., 2010] to handle the nuclear norm rank regularization of the matrix of unobserved factors, and a gradient descent step [Friedman et al., 2010] with respect to the  $l_1$  regularization of the covariate space. It is important to note that both steps remain within the realm of convex optimization, making the computation computationally efficient.

The values of the regularization parameters  $\lambda_{L,H,\beta}$  are selected through cross-validation. To ensure that the estimation of the ATET produces precise potential outcomes under no treatment, we aim to find the  $\lambda_{L,H,\beta}$  values that minimize the prediction error for potential outcomes. To maintain independence from whether the null hypothesis holds or not, we restrict the cross-validation sample to the observations in the control state. For a specified number of folds  $K$ , we randomly draw  $K$  sets  $\mathcal{O}_k \subset \mathcal{O}$  with a size  $\frac{|\mathcal{O}_k|}{|\mathcal{O}|} = \frac{|\mathcal{O}|}{NT}$ , corresponding to the overall share of untreated observations. The evaluation set for each fold is given by  $\mathcal{O}_k^- := (i, t) : (i, t) \in \mathcal{O}, (i, t) \notin \mathcal{O}_k$ . For a chosen set  $\Lambda$ , we search for the optimal  $\lambda$ -configuration by minimizing the mean squared prediction error over all partitions as follows:

$$(\lambda_L, \lambda_H, \lambda_\beta) = \arg \min_{(\lambda_{L'}, \lambda_{H'}, \lambda_{\beta'}) \in \Lambda} \sum_{k=1}^K \left\| \mathbf{P}_{\mathcal{O}_k^-} \left( \mathbf{Y} - \hat{\mathbf{L}}'_k - \mathbf{X} \hat{\mathbf{H}}'_k \mathbf{Z} - \left[ \mathbf{v}_{it}^\top \hat{\boldsymbol{\beta}}'_k \right]_{it} - \hat{\boldsymbol{\Gamma}}'_k \mathbf{1}_T^\top - \mathbf{1}_N (\hat{\boldsymbol{\Delta}}'_k)^\top \right) \right\|_F^2.$$

Here,  $(\hat{\mathbf{L}}'_k, \hat{\mathbf{H}}'_k, \hat{\boldsymbol{\beta}}'_k, \hat{\boldsymbol{\Gamma}}'_k, \hat{\boldsymbol{\Delta}}'_k)$  are estimated by (6) on each training set  $\mathcal{O}_k$  using the penalty parameters  $(\lambda_{L'}, \lambda_{H'}, \lambda_{\beta'})$ .

To restrict the set of to-be-evaluate elements  $\Lambda$ , we identify the theoretical minimal values of  $\lambda_{L,H,\beta}$  such that all parameter estimates in the respective objects are reduced to 0. Along with  $\lambda_{L,H,\beta} = 0$ , this establishes two natural bounds for each penalization parameter. The optimization search can be conducted on a standard three-dimensional grid. The MCMS R-

package utilizes a more advanced hyper-cube search that leverages the convex optimization to expedite convergence to the minimizing configuration. This approach enhances the efficiency of the parameter selection process.

A natural extension of estimators with integrated model selection is to implement a two-stage procedure. In the first stage, the estimation procedure is run as usual to identify the sparse model, and in the second stage, the estimation is performed without regularization on the identified subset of covariates [Chernozhukov et al., 2015]. The objective of the second stage is to obtain an unbiased estimate of model parameters by dropping the regularization. For the matrix completion method, the analogous two-stage estimator first identifies the informative covariates and determines the rank of  $\mathbf{L}$  in the first step. Then, in the second step, it applies an unregularized estimation under the restrictions on the covariate space and the rank of the factor model.

The estimation of the model (6) is obviously biased if the null hypothesis is violated. In such cases, the treatment effect might be either evenly dispersed over all observations and periods or allocated to confounding variables, leading to a reduction in the ATET estimate. If the assessment of p-values is not a need, an estimation of the model parameters using only the observations in the absence of treatment yields more precise estimates of the treatment effect:

$$\begin{aligned}
 (\hat{\mathbf{L}}, \hat{\mathbf{H}}, \hat{\boldsymbol{\beta}}, \hat{\boldsymbol{\Gamma}}, \hat{\boldsymbol{\Delta}}) = \arg \min_{\mathbf{L}, \mathbf{H}, \boldsymbol{\beta}, \boldsymbol{\Gamma}, \boldsymbol{\Delta}} \left\{ \frac{1}{|\mathcal{O}|} \left\| \mathbf{P}_{\mathcal{O}} (\mathbf{Y} - \mathbf{L} - \mathbf{X}\mathbf{H}\mathbf{Z} - [\mathbf{V}_{it}^{\top} \boldsymbol{\beta}]_{it} - \boldsymbol{\Gamma} \mathbf{1}_T^{\top} - \mathbf{1}_N (\boldsymbol{\Delta})^{\top}) \right\|_F^2 \right. \\
 \left. + \lambda_L \|\mathbf{L}\|_* + \lambda_H \|\mathbf{H}\|_{1,e} + \lambda_{\beta} \|\boldsymbol{\beta}\|_{1,e} \right\},
 \end{aligned} \tag{7}$$

It is important to note that if the treatment effect is independent of the covariates or the unconfoundedness assumption holds, the treatment effect is distributed evenly across all observations. Under the assumption of an independent treatment effect, each observation receives a share of the average effect among the treated sample, given by  $\frac{|\mathcal{M}|}{|\mathcal{O}|}$ . If we assume homogeneity, this share is equal to the ATET. However, in situations with strongly heterogeneous treatment effects, the average effect in the sample may diverge from the ATET.

Additionally, the treatment allocation mechanism also affects the dispersion of treatment effects among the observations under the unconfoundedness assumption. The split of the sample average effect assigns more weight to observations with a higher propensity score, as the treatment effect is partly allocated to confounding variables. To correct the ATET for marginal treatment effect and propensity score heterogeneity, a simple rule-of-thumb correction is given by:

$$\hat{\tau}_{\text{ATET,rot.cor}} = \frac{NT}{|\mathcal{O}|} \hat{\tau}_{\text{ATET}} \quad (8)$$

### 3 Theoretical properties

**Definition 1** (Definition of test statistic  $S$ ). *The test statistic  $S(\hat{U})$  is defined as follows:*

$$S(\hat{U}) = |\mathcal{M}|^{-1} \sum_{(i,t) \in \mathcal{M}} |\hat{U}_{it}|$$

While other test statistics based on element-wise p-norms are theoretically possible, the test statistic in Definition 1 has been found to exhibit good properties when estimating average treatment effects [Chernozhukov et al., 2021].

**Assumption 3** (Bounded test statistic). *Assume that, under the null hypothesis, the density function of the test statistic  $S(U)$  exists and is bounded.*

Let the actual and estimated shock-discarded potential outcomes in the absence of treatment be denoted as:

$$\begin{aligned} \mathbf{Y}^{0,\varepsilon} &:= \mathbf{L}^* + \mathbf{X}\mathbf{H}^*\mathbf{Z} + [\mathbf{V}_{it}^\top \boldsymbol{\beta}^*]_{it} + \boldsymbol{\Gamma}^* \mathbf{1}_T^\top + \mathbf{1}_N (\boldsymbol{\Delta}^*)^\top = \mathbf{Y}(0) - \mathbf{U} \\ \hat{\mathbf{Y}}^{0,\varepsilon} &:= \hat{\mathbf{L}} + \mathbf{X}\hat{\mathbf{H}}\mathbf{Z} + [\mathbf{v}_{it}^\top \hat{\boldsymbol{\beta}}]_{it} + \hat{\boldsymbol{\Gamma}} \mathbf{1}_T^\top + \mathbf{1}_N (\hat{\boldsymbol{\Delta}})^\top = \hat{\mathbf{Y}}(0) \end{aligned}$$

**Assumption 4** (Consistency of the counterfactual estimation). *Suppose that  $\hat{\mathbf{Y}}^{0,\varepsilon}$  is a mean-unbiased predictor of  $\mathbf{Y}^{0,\varepsilon}$ . Let there be two sequences  $\gamma_{N,T}, \delta_{N,T}$  converging to 0 in  $NT$ . Assume with probability  $1 - \gamma_{N,T}$  that*

1.  $(NT)^{-1} \left\| \hat{\mathbf{Y}}^{0,\varepsilon} - \mathbf{Y}^{0,\varepsilon} \right\|_2^2 \leq \delta_{N,T}^2$  (small estimation mse), and

2.  $\forall_{(i,t) \in \mathcal{O}} : \left| \hat{\mathbf{Y}}^{0,\varepsilon} - \mathbf{Y}^{0,\varepsilon} \right| \leq \delta_{N,T}$  (small pointwise estimation error).

Assumption 4 is easy to verify for various types of estimators, including the basic non-regularized version of the matrix completion estimator, as shown in Chernozhukov et al. [2021]. The following lemma elaborates on the primitive conditions to ensure that the proposed estimator with covariate regularization satisfies Assumption 4.

**Lemma 1.** *Consider the Estimator (6) and assume the conditions stated at the beginning of the proof, then  $(NT)^{-1} \left\| \hat{\mathbf{Y}}^{0,\varepsilon} - \mathbf{Y}^{0,\varepsilon} \right\|_2^2 = o_P(1)$  and  $\forall_{(i,t) \in \mathcal{M}} : \left| \hat{\mathbf{Y}}_{it}^{0,\varepsilon} - \mathbf{Y}_{it}^{0,\varepsilon} \right| = o_P(1)$ .*

We make use of permutations to compute the p-values.

**Definition 2** (Set of permutations). *If Assumption 2.1 holds, a permutation is a one-to-one mapping  $\pi : \{1, \dots, N\} \times \{1, \dots, T\} \mapsto \{1, \dots, N\} \times \{1, \dots, T\}$ . In case of Assumption 2.2, a permutation is the set of horizontal moving block permutations for each individual  $\pi = \{\pi_i^{t'}\}_{i=1}^N$  where the respecting observation-internal moving block permutation is defined as*

$$\pi_{t'}(t) = \lfloor t + t' \rfloor_T$$

The set of all possible permutations is denoted by  $\Pi$ . For each  $\pi \in \Pi$ , we define the matrix of permuted residuals  $\hat{U}_\pi := \left[ \hat{U}_{\pi(i,t)} \right]_{i,t}$ , or  $\hat{U}_\pi := \left[ \hat{U}_{i,\pi(t)} \right]_{i,t}$  respectively.

For the finite sample validity of the matrix completion estimator, the choice of  $\Pi$  is irrelevant. However it is worth to note that set of one-to-one mappings on  $\{1, \dots, N\} \times \{1, \dots, T\}$  is larger than the set of horizontal moving block permutations allowing for the computation of more precise p-values under Assumption 2.1.

**Definition 3** (Definition of p-value). *The p-value is defined as*

$$\hat{p} = 1 - \hat{F} \left( S(\hat{U}) \right), \text{ where } \hat{F}(x) = \frac{1}{|\Pi|} \sum_{\pi \in \Pi} \mathbf{1} \left\{ S \left( \hat{U}_\pi \right) < x \right\}$$

**Theorem 1** (Approximate validity of p-value). *Suppose that Assumptions 2-4 hold. Then under the null hypothesis, the p-value is approximately unbiased in size:*

$$|P[\hat{p} \leq \alpha] - \alpha| \leq C(\tilde{\delta}_{N,T} + \delta_{N,T} + \sqrt{\delta_{N,T}} + \gamma_{N,T})$$

where  $\tilde{\delta}_{N,T} = (|\mathcal{M}|/|\mathcal{O}|)^{1/4}(\log(NT))$  and the constant  $C$  depends on  $|\mathcal{M}|$  but not on  $N$  and  $T$ .

Note that the results of Theorem 1 are non-asymptotic, i.e. they hold in finite sample. The finite sample bounds of the size properties imply that the inference procedure is exact in  $NT \rightarrow \infty$ . Naturally, the power of the hypothesis testing depends on characteristics of the underlying model (2). For instance, if the model is estimated more accurately or if the shocks have a smaller variance, the hypothesis tests tend to have higher power.

## 4 Simulation

In the following section, the results are only presented for matrix  $\mathbf{H}$  that links the unit-specific and the time-specific covariates. All findings equivalently apply for  $\beta$ , the parameter of the unit-time-varying covariates. The corresponding figures are presented in Appendix E.

### 4.1 Data-generating process

For the subsequent simulations, we use the following data-generating process: The outcome matrix follows the linear model in (2) with a homogeneous treatment effect<sup>6</sup>, interactive unit- and time-specific covariates, unit-time varying covariates, unit fixed-effects and time fixed-effect terms. The treatment allocation  $\mathbf{W}$  follows a Bernoulli model. The latent factor model matrix  $\mathbf{L}$  is random matrix restricted to a specified  $\text{rank}_L$  with exponentially distributed singular values. The unit-specific covariates of size  $p$  are multi-variate normal with an idiosyncratic unit factor, time-specific covariates of size  $q$  are generated accordingly. The coefficients of  $\mathbf{H}$ , the link between those covariates, are normally distributed, but only a random fraction is *active* while the other elements are set to 0. The data-generating process omits linear terms in the unit- or time-specific covariates as discussed in Section 2. The unit-

---

<sup>6</sup>The matrix completion estimator can naturally deal with heterogeneous treatment effects. As our object of interest is the average treatment effect on the treated, we stay with homogeneous effects for the simulation.

time varying covariates  $\mathbf{V}_{it}$  are independent standard normal and of the true coefficients  $\boldsymbol{\beta}$ , again, only a fraction is active.

The exact formulations of all components and the default parameter values are described in Appendix C.

## 4.2 Choice of optimal penalty parameters by cross-validation

Figure 1 shows the paths of the estimated coefficients in  $\hat{\mathbf{H}}$  for different values of  $\lambda_H$ . We observe the known pattern of  $l_1$  regularisation that coefficients with small attributed parameter values are wiped out for already low penalty parameters. With increasing regularization, one variable by another is eliminated until even the variables with largest absolute coefficient estimates are regularized out. The descriptive illustrations on the size and the number of coefficient parameters in Appendix D.1 confirm that the elimination process closely follows the order of parameter estimates in the absence of very strong correlation patterns among the covariates.

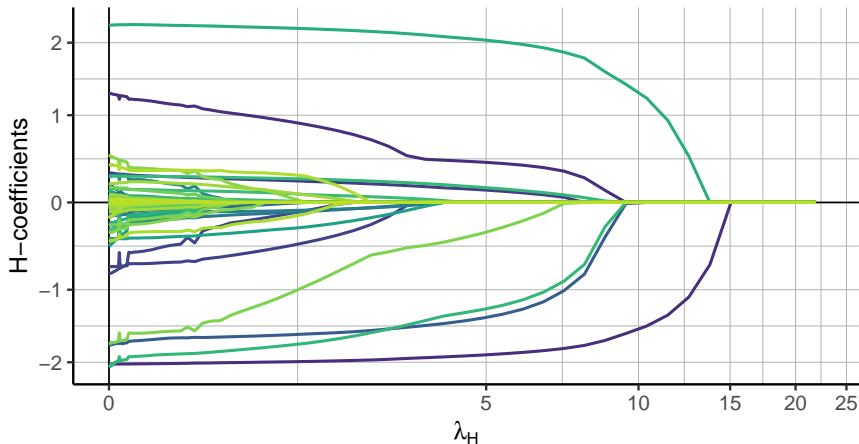


Figure 1: Path of estimated coefficients in  $\hat{\mathbf{H}}$  for different values of regularization parameter  $\lambda_H$

As discussed in Section 2, the optimal values of the penalty parameters  $(\lambda_L, \lambda_H, \lambda_\beta)$  are chosen by cross-validation. Figure 2 shows the mean prediction error on the test sample over the cross-validation folds for different values of the regularization parameter  $\lambda_H$ . The

convex optimization along the penalization parameter clearly shows itself.

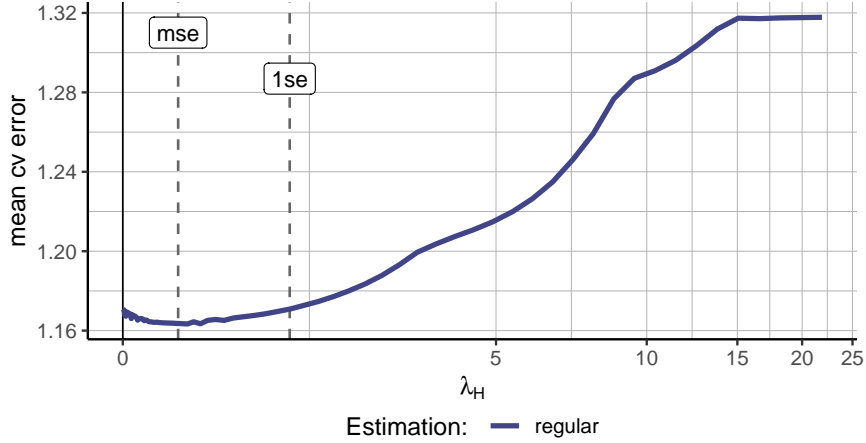


Figure 2: Mean error of out-of-sample prediction over cross-validation folds of  $\hat{\mathbf{H}}$  for different values of regularization parameter  $\lambda_H$

Note: 'mse' and '1se' show determined  $\lambda_H$  based on *mse* and *1se* optimality criteria.

As in each fold, the objective function is only evaluated on a subsample of the available data, the cross-validation optimization is not necessarily optimal for the out-of-sample observations. A known issue is the estimation error of risk curves using cross-validation samples [Hastie et al., 2009]. Because of this estimation error, model selection using cross-validation tends to be too conservative while in fact, the smallest model is preferred among a set of indistinguishable models [Chen and Yang, 2021]. To address this, we implement the common *1se* solution, which selects for the largest value of the penalization parameter for which the objective function remains below the minimum value plus one standard error over the cross-validation folds calculated at the optimal  $\lambda_H$  position. The results on the number and size of the non-zero coefficients in Appendix D.1 strongly support the application of the *1se* solution.

### 4.3 Accuracy of treatment effect estimates

In this subsection, we evaluate the estimation error over multiple samples to remove the dependency of the measured estimation error on a specific randomly generated sample. The

plots in the subsequent subsections use the abbreviation as described in Table 1 to denote different estimation methods.

Table 1: Abbreviation for estimation methods

<i>no_reg</i>	Estimation as in Athey et al. [2021] without any covariate regularization.
<i>imp0</i>	Estimation with covariate regularization with imposed null hypothesis.
<i>imp0_rot</i>	<i>imp0</i> estimation using the rule-of-thumb correction.
<i>imp0_post</i>	Two-stage estimation with model/rank-selection from 'imp0' estimation and unregularized post step.
<i>imp0_lse</i>	<i>imp0</i> estimation using 'lse' optimality criterion in cross-validation.
<i>not0</i>	Estimation with covariate regularization without imposing the null hypothesis. (Does not allow for inference on effect estimates)

Figure 3 shows the boxplot of ATET estimates by different sample sizes for the six versions of the matrix completion estimator as outlined in Table 1. All estimators using covariate regularization perform a great deal better, in particular for small sample sizes. However, the versions imposing the null hypothesis exhibit a substantial downward bias, which is the price paid for enabling the inference procedure. With a decent sample size, the rule-of-thumb correction is able to eliminate the bias. The matrix completion estimator without imposed null, as in Athey et al. [2021], but using covariate regularization is unbiased and performs already excellently for very small sample sizes.

The fit of the post-regularization model is consistently very poor. It can be shown that the estimates of  $\hat{\mathbf{L}}$  are closely tied to the regularization by the penalty term. When dropping the penalization parameter in the post-regularization step, the coefficient in  $\hat{\mathbf{L}}$  strongly diverge from the true values.

To undertake the estimation accuracy in a more detailed evaluation, Figure 4 shows the median indexed squared error of the treatment effect where the squared errors in each sample are divided by the squared estimation error of the baseline *imp0* estimator. Hence, a value below 1 denotes that an estimator performs on average better than the basic regularized



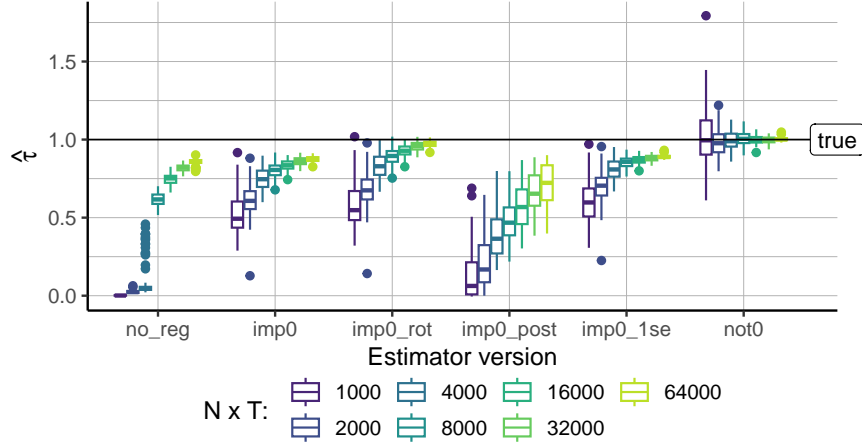


Figure 3: Boxplot of  $\hat{\tau}$  by estimation method.

Note:  $N = 100$ ,  $T \in \{10, 20, 40, 80, 160, 320, 640\}$ . 700 runs per sample size. True value of  $\tau = 1$ .

estimator with imposed null.<sup>7</sup> This illustration refines and accentuates the insights from Figure 3 that the enabled inference procedure by imposing the null hypothesis comes at a substantial price in treatment effect estimation accuracy. With increasing sample size, the rule-of-thumb correction achieves similar precision as the matrix completion estimator without the null hypothesis imposed. Thus, if inference on the treatment effect estimator is desired, applying the rule-of-thumb correction can partially compensate for the accuracy loss by the implied null hypothesis for the inference procedure.

The simulation results further evince that the reduction in model size confers benefits to estimation accuracy, particularly in the context of small sample sizes. The lower degrees of freedom of the fitted model result in better predictions for the potential outcomes under no-treatment of the treated observations with the available data. For larger sample sizes, there is enough information in the data such that fitting the full model without covariate regularization picks up less spurious correlations of non-explanatory covariates such that the estimation accuracy levels with the regularized version of the estimator. Nevertheless, the gains in accuracy achieved through by applying the estimate correction or performing an estimation without inference are still massive compared to the unregularized estimation.

<sup>7</sup>Note that the median indexed squared error is an aggregate of a ratio and has to be interpreted accordingly.

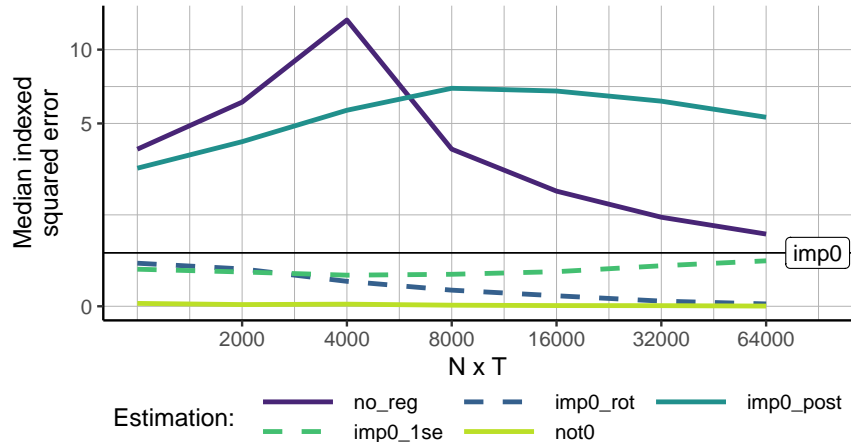


Figure 4: Median indexed squared error of  $\hat{\tau}$  by estimator version.

Note: *Indexed* measures are divided by the squared estimation error of the *imp0* model.  $N = 100$ ,  $T \in \{10, 20, 40, 80, 160, 320, 640\}$ . 700 runs per sample size. Transformed y-axis.

In Appendix D.2, we demonstrate that the bias of the treatment effect estimates is not negatively affected by a low signal-to-noise ratio, in fact, the bias is slightly decreasing for weaker signals. However, for a low signal-to-noise ratio, the variance of the treatment effect estimate is substantial. The relative performance of the different estimator versions reflects the pattern observed in Figures 3 and 4: The estimator without imposing the null hypothesis is superior for all settings and the rule-of-thumb correction *imp0\_rot* is consistently the best-performing estimator among the null hypothesis versions, in particular for low signal-to-noise ratios.

#### 4.4 Model selection property

We assess the dimensions of the ascertained model, defined by the count of non-zero coefficients in the matrix  $\mathbf{H}$ , in comparison to the true size of the generated sample across varying sample sizes. It is pertinent to note that the post-regularization and rule-of-thumb correction estimates have no impact on the model size. Consequently, we display only the unregularized estimation, the regularization approach employing *mse* and *lse* optimality criterion, and the estimator not imposing the null hypothesis.

Figure 5 illustrates a substantial reduction in the number of non-zero coefficients within

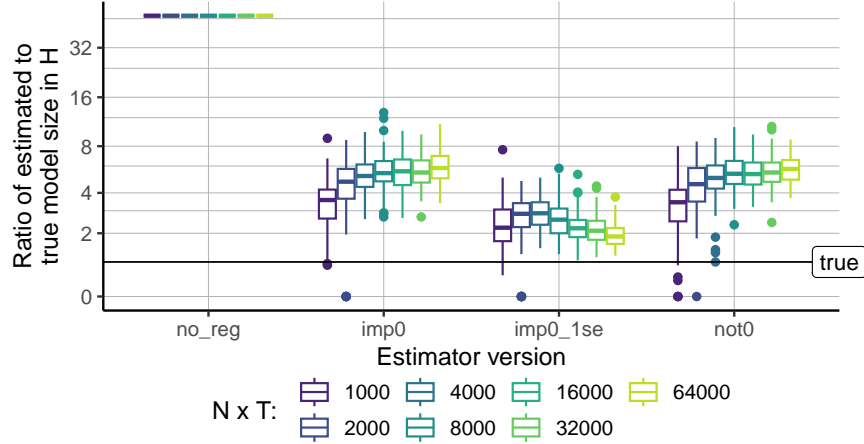


Figure 5: Ratio between the estimated and true model size in  $\mathbf{H}$ .

Note:  $N = 100$ ,  $T \in \{10, 20, 40, 80, 160, 320, 640\}$ . 700 simulations per sample size. The number of non-zero elements is equal for regular, rule-of-thumb correction, and post-regularization estimation. Transformed y-axis.

the estimated matrix  $\mathbf{H}$  when utilizing a regularized estimator.<sup>8</sup> Notably, the MSE-optimal cross-validation results in an overestimation, maintaining approximately five times the number of covariates within the determined model across all sample sizes. Conversely, the 1se variant consistently selects a model size that closely aligns with the true model size. As the sample size increases, there appears to be a convergence of the estimated model size towards the true value.

Additionally, in Appendix D.3, we provide evidence that the MSE of the estimated coefficients in  $\mathbf{H}$  exhibits a strong decrease as the sample size diminishes. The concurrent enhancements in both model size and coefficient accuracy contribute to the augmented precision in treatment effect estimates for larger sample sizes which has been observed in Section 4.3.

In Appendix D.4, we illustrate that the determined model size persists is stable as the signal exhibits substantial strength. Nevertheless, as the signal-to-noise ratios approach very small magnitudes, rendering the task of segregating relevant information from noise more difficult, all estimators tend to identify a reduced number of informative parameters within

<sup>8</sup>It is worth acknowledging that the actual count of non-zero coefficients in  $\mathbf{H}$  may deviate from the DGP parameter  $h_{\text{size}}$  under conditions where  $p < \bar{p}$  or  $q < \bar{q}$ .

the model. This discernment, in turn, can lead to estimated models that are more sparse than the true model.

## 5 Illustration

To showcase the usefulness of the proposed estimator in an empirical context, we apply the developed methodology to scrutinize the impact of governmental regulations aimed at mitigating the Covid-19 pandemic. The period encompassing the peak of the global pandemic witnessed an intense public discourse regarding the appropriateness and effectiveness of public health measures designed to curb the spread of SARS-CoV-2. This discourse extended into the academic domain, putting forth extensive evaluations of, e.g., governmental responses to the pandemic [Christensen et al., 2023, Basseal et al., 2023] or public compliance with health regulations [Scandurra et al., 2023].

In this illustrative analysis, we delve into the effect of international travel restrictions, a measure identified as highly effective by Basseal et al. [2023]. Our focus is on providing a pure analytical assessment of travel restrictions as a public health intervention. The geopolitical implications of travel bans and the suspension of visa exemptions are thoughtfully explored in Seyfi et al. [2023].

We analyze the impact of Covid-19 testing obligations upon entry from foreign countries with elevated incidence rates on the frequency of infections necessitating treatment in intensive care units (ICU). The testing obligation at entry from high-risk regions was partially implemented in Germany from the summer of 2020 to the spring of 2022.<sup>9</sup> To circumvent distortions in the outcome measure arising from limited testing capacities during the early stages of the pandemic, we confine the sample period to July 2020 to June 2022, utilizing weekly frequency. Additionally, to ensure robustness in our outcome measure, we exclude

---

<sup>9</sup>The authority for public health regulations in Germany has been dispersed to various administrative levels with a general trend to transition from individual districts to state-harmonized policies over time. Some regions temporarily intensified regulations by imposing testing obligations on all incoming travellers, which is not being distinguished in this analysis.

districts with fewer than 10 intensive care beds. It is noteworthy that, in the remaining districts, no district operated at maximum ICU occupancy for a significant duration, ensuring consistent reporting and treatment within the same district. With these restrictions, our analysis spans a panel of 342 units over 105 time periods.

The adoption of the ratio between patients treated in ICU due to Covid-19 infections and the number of reported infections as the outcome is appealing for two reasons. Firstly, travel restrictions primarily aim to avert the overwhelming strain on medical facilities by delaying the introduction of new and potentially threatening virus mutations. This delay allows more time for the refinement of vaccines to address emerging variants. Secondly, utilizing the frequency of severe infections as the outcome mitigates common concerns related to endogeneity and reverse causality when using plain incidence rates or vaccination rates as outcomes.<sup>10</sup>

Given the extensive research on the medical, economic, and social impact of the pandemic, comprehensive macroeconomic data is available for the selected time frame. The German Corona-Datenplattform<sup>11</sup> serves as a primary data source, offering a rich collection of macroeconomic, infection, and policy data. The dataset encompasses 91 unit-time-specific covariates (encompassing various public health regulations, vaccination prevalence, and short-time work data), 55 unit-specific covariates (encompassing socio-demographics, medical care, infrastructure, and economic composition variables), and 11 time-specific covariates (covering general economic indicators, mobility, tourism, and the prevalence of threatening mutations among all reported infections). The complete datasets, along with a detailed description of all variables, can be accessed on the Harvard Dataverse [Heiniger, 2024] related to this project.

---

<sup>10</sup>The median duration of ICU treatment for Covid-19 patients is between 10 to 14 days and exhibits a right-skewed distribution [Shryane et al., 2020, Kaçmaz et al., 2023]. Consequently, during periods of declining infection rates, the ratio of patients admitted to the ICU to the reported incidence may exceed 1. A direct mapping of ICU patients to an infection is not possible. Consequently, the metric employed in this study should be interpreted as a proxy for the severity of infections. For a more comprehensive examination of the epidemiological landscape extending this illustrative example, the adoption of more sophisticated metrics becomes requisite.

<sup>11</sup><https://www.healthcare-datenplattform.de/>

The provided context and dataset serve to exemplify the estimation and model selection characteristics of the proposed estimator within an empirical application. The application of the panel data model (2) requires the estimation of 1143 parameters.<sup>12</sup> Table 2 summarizes the estimation outcomes and resultant model sizes across the various versions of the estimator, denoted by previously introduced abbreviations detailed in Table 1. Notably, the estimated treatment effects are very close to 0. The p-values, approaching unity for the regularized estimators with imposed null hypothesis, suggest an increased precision in estimating potential outcomes for treated observations. This poses a challenge to the regularity assumption of the stochastic shock, as outlined in Assumption 2. Given the non-rejection of the hypothesis asserting the absence of a treatment effect, there is no compelling argument to accord greater credibility to the results obtained through the *not0* estimation procedure.

Table 2: Estimation results and model sizes by estimator version

	<i>no_reg</i>	<i>imp0</i>	<i>imp0_1se</i>	<i>not0</i>	<i>not0_1se</i>
ATET	0.00007	0.00014	0.00550	-0.00052	0.00674
ATET <sub>rot</sub>	0.00007	0.00015	0.00586	-	-
p-value	0.496	0.98	1	-	.
$\hat{\mathbf{H}}$ size	605	107	1	2	1
$\hat{\boldsymbol{\beta}}$ size	91	0	0	0	0
$\hat{\mathbf{L}}$ rank	25	76	1	71	1

Note: The model size is determined by the number of non-zero elements in  $\hat{\mathbf{H}}$  and  $\hat{\boldsymbol{\beta}}$ , as well as the number of singular values of  $\hat{\mathbf{L}}$ .

The lower segment of Table 2 elucidates the resultant model sizes derived from the estimation process. Notably, the *no\_reg* estimation, which solely regularizes the rank of the unobserved factor matrix  $\mathbf{L}$  while leaving covariates unpenalized, manifests the full model in terms of  $\mathbf{H}$  and  $\boldsymbol{\beta}$  parameters.<sup>13</sup> Estimators integrating covariate regularization substantially reduce the model size, yielding an exceedingly sparse model with merely one covariate when

<sup>12</sup>An extension of the model to (3), which incorporates linear terms in  $\mathbf{X}$  and  $\mathbf{Z}$ , expands the parameter count to 10,678. While technically feasible, estimating this augmented model is deemed impractical due to the exceedingly small signal-to-noise ratio within the specified application setting.

<sup>13</sup>Recall that the fixed effects remain unregularized throughout.

employing the *lse*-criterion. This observation suggests the presence of very weak signal influencing the severity of Covid-19 infection trajectories within the variables of the dataset. The single parameter persisting the model selection process links the proportion of students and the proportion of infections attributed to the Alpha variant (B.1.1.7) of the Covid-19 virus. These findings hint at a notable association between this mutation and an increased incidence of patients necessitating intensive care unit (ICU) treatment, with young individuals in educational settings possibly serving as significant channel for viral transmission. However, it is essential to underscore that this interpretation hinges solely on the interpretation of model parameters and does not denote an identified causal effect.

## 6 Conclusion

We present novel findings concerning  $l_1$  covariate regularization within matrix completion methods. A comprehensive simulation study illustrates that this form of regularization significantly diminishes the model size. The determination of penalization parameters through cross-validation, employing the *lse* optimality criterion, yields a model size that converges to the true value as the panel size increases.

Moreover, we establish the applicability of the permutation-based inference procedure proposed by Chernozhukov et al. [2021] to the extended estimator incorporating covariate regularization. Additionally, we demonstrate its validity under any treatment assignment mechanism. While enforcing the null hypothesis of a treatment effect absence, a prerequisite for applying the inference procedure, introduces a downward bias in effect estimates, simulation results indicate that this bias can be substantially reduced, and even completely mitigated for larger sample sizes, through a simple rule-of-thumb correction.

The proposed estimator, utilizing both *lse*-regularization and the estimate correction when inference is necessary, displays superior prediction accuracy compared to the baseline matrix completion estimator introduced by Athey et al. [2021]. The latter has been demon-

strated to outperform other common estimators in panel data regression methods. Apart from improved treatment effect estimates, our proposed estimator additionally features a robust model selection property and enables valid finite sample inference.

Future research avenues may include enhancing the two-stage procedure by integrating a more suitable post-model-selection estimation. The application of matrix completion methods in the second step, as evidenced by our simulation study, results in inferior prediction accuracy. Another potential direction for future work involves incorporating an alternative inference procedure that does not impose bias on treatment effect estimates. For instance, a Bayesian inference approach simulating posterior draws via a Markov Chain Monte Carlo sampler, as proposed by Tanaka [2021], could be explored.

Additionally, our proposed estimator can be linked to the broader literature that facilitates the application of matrix completion methods to patterns of missing data that are not completely random, as explored by Bhattacharya and Chatterjee [2022], Agarwal et al. [2021], and Bai and Ng [2021].

## References

- A. Abadie and J. Gardeazabal. The economic costs of conflict: A case study of the basque country. *American Economic Review*, 93(1):113–132, March 2003. doi: 10.1257/000282803321455188. URL <https://www.aeaweb.org/articles?id=10.1257/000282803321455188>.
- A. Abadie, A. Diamond, and J. Hainmueller. Synthetic control methods for comparative case studies: Estimating the effect of california’s tobacco control program. *Journal of the American statistical Association*, 105(490):493–505, 2010.
- A. Agarwal, M. Dahleh, D. Shah, and D. Shen. Causal matrix completion, 2021.



- M. Amjad, D. Shah, and D. Shen. Robust synthetic control. *The Journal of Machine Learning Research*, 19(1):802–852, 2018.
- D. Arkhangelsky and G. W. Imbens. Doubly robust identification for causal panel data models. *The Econometrics Journal*, 25(3):649–674, 06 2022. ISSN 1368-4221. doi: 10.1093/ectj/utac019. URL <https://doi.org/10.1093/ectj/utac019>.
- D. Arkhangelsky, S. Athey, D. A. Hirshberg, G. W. Imbens, and S. Wager. Synthetic difference-in-differences. *American Economic Review*, 111(12):4088–4118, 2021.
- S. Athey, M. Bayati, G. Imbens, and Z. Qu. Ensemble methods for causal effects in panel data settings. In *AEA Papers and Proceedings*, volume 109, pages 65–70. American Economic Association 2014 Broadway, Suite 305, Nashville, TN 37203, 2019.
- S. Athey, M. Bayati, N. Doudchenko, G. Imbens, and K. Khosravi. Matrix completion methods for causal panel data models. *Journal of the American Statistical Association*, 116(536):1716–1730, 2021.
- J. Bai. Inferential theory for factor models of large dimensions. *Econometrica*, 71(1):135–171, 2003.
- J. Bai and S. Ng. Matrix completion, counterfactuals, and factor analysis of missing data. *Journal of the American Statistical Association*, 116(536):1746–1763, 2021.
- J. Basseal, C. Bennett, P. Collignon, B. Currie, D. Durrheim, J. Leask, E. McBryde, P. McIntyre, F. Russell, D. Smith, et al. Key lessons from the covid-19 public health response in australia. *The Lancet Regional Health–Western Pacific*, 30, 2023.
- A. Belloni and V. Chernozhukov. Least squares after model selection in high-dimensional sparse models. *Bernoulli*, pages 521–547, 2013.
- A. Belloni, V. Chernozhukov, and C. Hansen. Inference on treatment effects after selection among high-dimensional controls. *The Review of Economic Studies*, 81(2):608–650, 2014.

- A. Belloni, V. Chernozhukov, I. Fernández-Val, and C. Hansen. Program evaluation and causal inference with high-dimensional data. *Econometrica*, 85(1):233–298, 2017.
- E. Ben-Michael, A. Feller, and J. Rothstein. The augmented synthetic control method. *Journal of the American Statistical Association*, 116(536):1789–1803, 2021.
- S. Bhattacharya and S. Chatterjee. Matrix completion with data-dependent missingness probabilities. *IEEE Transactions on Information Theory*, 68(10):6762–6773, 2022.
- B. Callaway and P. H. Sant’Anna. Difference-in-differences with multiple time periods. *Journal of Econometrics*, 225(2):200–230, 2021.
- E. Candes and B. Recht. Exact matrix completion via convex optimization. *Communications of the ACM*, 55(6):111–119, 2012.
- E. J. Candes and Y. Plan. Matrix completion with noise. *Proceedings of the IEEE*, 98(6):925–936, 2010.
- Y. Chen and Y. Yang. The one standard error rule for model selection: Does it work? *Stats*, 4(4):868–892, 2021. ISSN 2571-905X. doi: 10.3390/stats4040051. URL <https://www.mdpi.com/2571-905X/4/4/51>.
- V. Chernozhukov, C. Hansen, and M. Spindler. Valid post-selection and post-regularization inference: An elementary, general approach. *Annu. Rev. Econ.*, 7(1):649–688, 2015.
- V. Chernozhukov, K. Wüthrich, and Y. Zhu. An exact and robust conformal inference method for counterfactual and synthetic controls. *Journal of the American Statistical Association*, 116(536):1849–1864, 2021.
- T. Christensen, M. D. Jensen, M. Kluth, G. H. Kristinsson, K. Lynggaard, P. Læg Reid, R. Niemikari, J. Pierre, T. Raunio, and G. Adolf Skúlason. The nordic governments’ responses to the covid-19 pandemic: A comparative study of variation in governance arrangements and regulatory instruments. *Regulation & Governance*, 17(3):658–676,

2023. doi: <https://doi.org/10.1111/rego.12497>. URL <https://onlinelibrary.wiley.com/doi/abs/10.1111/rego.12497>.
- C. De Chaisemartin and X. d'Haultfoeuille. Two-way fixed effects estimators with heterogeneous treatment effects. *American Economic Review*, 110(9):2964–2996, 2020.
- J. Fan and R. Li. Statistical challenges with high dimensionality: Feature selection in knowledge discovery. *arXiv preprint math/0602133*, 2006.
- J. Fan, K. Li, and Y. Liao. Recent developments in factor models and applications in econometric learning. *Annual Review of Financial Economics*, 13(1):401–430, 2021. doi: 10.1146/annurev-financial-091420-011735.
- M. H. Farrell. Robust inference on average treatment effects with possibly more covariates than observations. *Journal of Econometrics*, 189(1):1–23, 2015.
- I. Fernández-Val, H. Freeman, and M. Weidner. Low-rank approximations of nonseparable panel models. *The Econometrics Journal*, 24(2):C40–C77, 03 2021. ISSN 1368-4221. doi: 10.1093/ectj/utab007. URL <https://doi.org/10.1093/ectj/utab007>.
- J. Friedman, T. Hastie, and R. Tibshirani. Regularization paths for generalized linear models via coordinate descent. *Journal of statistical software*, 33(1):1, 2010.
- A. Goodman-Bacon. Difference-in-differences with variation in treatment timing. *Journal of Econometrics*, 225(2):254–277, 2021.
- T. Hastie, R. Tibshirani, J. H. Friedman, and J. H. Friedman. *The elements of statistical learning: data mining, inference, and prediction*, volume 2. Springer, 2009.
- S. Heiniger. MCMS, 2024. URL <https://doi.org/10.7910/DVN/JGGBQG>.
- X. Jin, B. W. Wah, X. Cheng, and Y. Wang. Significance and challenges of big data research. *Big data research*, 2(2):59–64, 2015.

- B. Kaçmaz, Ş. Keske, U. Sişman, S. T. Ateş, M. Güldan, Y. Beşli, E. Palaoğlu, N. Çakar, and Ö. Ergönül. Covid-19 associated bacterial infections in intensive care unit: a case control study. *Scientific Reports*, 13(1):13345, 2023.
- M. Kellogg, M. Mogstad, G. A. Pouliot, and A. Torgovitsky. Combining matching and synthetic control to tradeoff biases from extrapolation and interpolation. *Journal of the American Statistical Association*, 116(536):1804–1816, 2021. doi: 10.1080/01621459.2021.1979562. PMID: 35706442.
- M. R. Kosorok. *Introduction to empirical processes and semiparametric inference*, volume 61. Springer, 2008.
- S. R. Künzel, J. S. Sekhon, P. J. Bickel, and B. Yu. Metalearners for estimating heterogeneous treatment effects using machine learning. *Proceedings of the national academy of sciences*, 116(10):4156–4165, 2019.
- R. Levy and M. Mattsson. The effects of social movements: Evidence from# metoo. *Available at SSRN 3496903*, 2022.
- W. Ma and G. H. Chen. Missing not at random in matrix completion: The effectiveness of estimating missingness probabilities under a low nuclear norm assumption. *Advances in neural information processing systems*, 32, 2019.
- R. Mazumder, T. Hastie, and R. Tibshirani. Spectral regularization algorithms for learning large incomplete matrices. *The Journal of Machine Learning Research*, 11:2287–2322, 2010.
- N. Meinshausen. Relaxed lasso. *Computational Statistics & Data Analysis*, 52(1):374–393, 2007.
- N. Meinshausen and P. Bühlmann. Variable selection and high-dimensional graphs with the lasso. *Ann Stat*, 34:1436–1462, 2006.

- Y. Ning, P. Sida, and K. Imai. Robust estimation of causal effects via a high-dimensional covariate balancing propensity score. *Biometrika*, 107(3):533–554, 2020.
- R. Rafaty, G. Dolphin, and F. Pretis. Carbon pricing and the elasticity of co2 emissions, 2020.
- B. Recht, M. Fazel, and P. A. Parrilo. Guaranteed minimum-rank solutions of linear matrix equations via nuclear norm minimization. *SIAM review*, 52(3):471–501, 2010.
- E. Rio et al. *Asymptotic theory of weakly dependent random processes*, volume 80. Springer, 2017.
- P. R. Rosenbaum and D. B. Rubin. The central role of the propensity score in observational studies for causal effects. *Biometrika*, 70(1):41–55, 1983.
- P. H. Sant’Anna and J. Zhao. Doubly robust difference-in-differences estimators. *Journal of Econometrics*, 219(1):101–122, 2020.
- C. Scandurra, V. Bochicchio, P. Dolce, P. Valerio, B. Muzii, and N. M. Maldonato. Why people were less compliant with public health regulations during the second wave of the covid-19 outbreak: The role of trust in governmental organizations, future anxiety, fatigue, and covid-19 risk perception. *Current Psychology*, 42(9):7403–7413, 2023.
- S. Seyfi, C. M. Hall, and B. Shabani. Covid-19 and international travel restrictions: the geopolitics of health and tourism. *Tourism Geographies*, 25(1):357–373, 2023.
- N. Shryane, M. Pampaka, A. Aparicio-Castro, S. Ahmad, M. J. Elliot, J. Kim, J. Murphy, W. Olsen, D. P. Ruiz, and A. Wiśniowski. Length of stay in icu of covid-19 patients in england, march-may 2020. *International Journal of Population Data Science*, 5(4), 2020.
- M. Tanaka. Bayesian matrix completion approach to causal inference with panel data. *Journal of Statistical Theory and Practice*, 15(2):49, 2021.

- R. Tibshirani. Regression shrinkage and selection via the lasso. *Journal of the Royal Statistical Society: Series B (Methodological)*, 58(1):267–288, 1996.
- M. Udell and A. Townsend. Why are big data matrices approximately low rank? *SIAM Journal on Mathematics of Data Science*, 1(1):144–160, 2019.
- G. Wood, T. R. Tyler, and A. V. Papachristos. Procedural justice training reduces police use of force and complaints against officers. *Proceedings of the National Academy of Sciences*, 117(18):9815–9821, 2020.
- Y. Xu. Generalized synthetic control method: Causal inference with interactive fixed effects models. *Political Analysis*, 25(1):57–76, 2017.
- H. Zou. The adaptive lasso and its oracle properties. *Journal of the American statistical association*, 101(476):1418–1429, 2006.

# A Background on matrix completion estimators in the context of causal panel data models

The econometric literature on panel data with binary treatment exposure has recently evolved in four main streams: The literature on unconfoundedness [Rosenbaum and Rubin, 1983] imputes data for missing potential outcomes using observed outcomes of comparable units in previous periods (See Arkhangelsky and Imbens [2022] for recent advances). The literature on synthetic control Abadie and Gardeazabal [2003], Abadie et al. [2010], Amjad et al. [2018], Ben-Michael et al. [2021], Kellogg et al. [2021] imputes missing potential outcomes by creating a hypothetical but representative control unit. The literature on factor (or interactive effects) models estimates unobserved outcomes as the sum of a low-rank factor structure and a linear function of covariates [Bai, 2003, Xu, 2017, Fan et al., 2021]. Finally, the difference-in-difference literature relies on the assumption that all average outcomes follow a parallel path over time in the absence of treatment [Sant’Anna and Zhao, 2020, De Chaisemartin and d’Haultfoeuille, 2020, Callaway and Sant’Anna, 2021, Goodman-Bacon, 2021, Arkhangelsky et al., 2021].

The suitability of the respective methods in a particular application is mainly determined by the structure of the data. For instance, the unconfoundedness literature typically applies to settings with a single treatment period, making it suitable for *horizontal* regression. On the other hand, the synthetic control literature is well-suited for settings with one (or few) treated units, making it a *vertical* regression framework. In horizontal regression, the focus is on stable patterns over time across units, while vertical regression relies on stable patterns over units across time.

The matrix completion method for causal panel data models builds upon the literature on factor models and demonstrates that both horizontal and vertical regression can be nested into the matrix completion objective function [Athey et al., 2021]. Similar to general factor models, the outcome model consists of an unobserved low-rank matrix plus noise, with an

optional linear covariate component. However, matrix completion methods [Mazumder et al., 2010, Candes and Plan, 2010, Candes and Recht, 2012, Fernández-Val et al., 2021] differ from factor model literature in how they determine the rank. While factor models estimate, bound, or assume the rank to be known, matrix completion methods determine the rank through regularization, using a penalty term in the objective function. Regularization is particularly suitable in causal panel data settings as the focus is on imputing missing elements in the matrix of potential outcomes rather than consistently estimating the underlying factors.

Matrix completion methods are typically constrained to cases where each observation has an independent and non-zero probability of being missing [Ma and Chen, 2019]. However, Athey et al. [2021] derived bounds for estimating the average treatment effect of the treated (ATET) in causal panel data models, even when the missing data patterns are not completely random.

To address the inference challenges across the various panel data literature streams, Chernozhukov et al. [2021] introduced a uniformly valid inference procedure applicable to matrix completion methods as well. Their permutation-based inference offers a generic and robust approach for settings with few treated units, with the treatment occurring uniformly for a defined number of periods at the end of the time interval, while accommodating stationary and weakly dependent shocks.

The efficiency of regularization on the nuclear norm of the unobserved factor matrix in matrix completion methods is closely related to the number of missing elements in the matrix. For instance, the convergence bounds in Athey et al. [2021] assume a maximum probability for missing elements per time-period, while Chernozhukov et al. [2021] requires the number of pre-treatment periods to be larger than the number of periods under treatment. In most applications, more observations are observed in a treated state, leading to a focus on estimating the average treatment effect of the treated (ATET) in causal analysis using matrix completion methods. However, in cases where there is a larger set of observations under treatment, the perspective can be switched accordingly.



## B Proofs

### B.1 Additional notation

We introduce additional notation that will be used in the proofs. For  $a, b \in \mathbb{R} : a \vee b := \max(a, b)$ . Without any subscript,  $\|\cdot\|$  denotes the Euclidian norm for vectors and the spectral norm for matrices.  $\lfloor a \rfloor$  rounds  $a$  down to the nearest integer.  $\lfloor a \rfloor_b$  denotes  $a \pmod{b}$ . The element-wise matrix multiplication (Hadamard product) is written as  $A \circ B$ . The maximal amount of treated time periods per observation is defined as  $|\mathcal{M}|_{\max} = \max_{1 \leq i \leq N} \sum_{1 \leq t \leq T} (i, t) \in \mathcal{M}$ .  $\mathcal{Z}$  denotes the set  $\{\mathbf{L}, \mathbf{X}, \mathbf{H}, \mathbf{Z}, \mathbf{V}, \beta\}$ . We rewrite the term  $\mathbf{X}\mathbf{H}\mathbf{Z}$  as a matrix-vector multiplications  $\mathbf{X}\mathbf{H}\mathbf{Z} = [\overline{\mathbf{X}\mathbf{Z}}_{it} \overline{\mathbf{H}}]_{it}$ , where the elements in  $\overline{\mathbf{H}}$  are the concatenated columns of  $\mathbf{H}$  and the entries in  $\overline{\mathbf{X}\mathbf{Z}}_{it}$  follow from the equality.

Note that, to shorten the notation of the subsequent proofs, we redefine the underlying model (2) by including the fixed effects term in the factor matrix  $\overline{\mathbf{L}} := \mathbf{L} + \mathbf{\Gamma}^* \mathbf{1}_T^\top + \mathbf{1}_N (\mathbf{\Delta}^*)^\top$ . This does not affect the low-rank assumption on  $\mathbf{L}$ . For ease of readability, we misuse the notation of  $\mathbf{L}$  by meaning  $\overline{\mathbf{L}}$ . Adaptations to the proofs using the true model (2) are straightforward.

### B.2 Proof of Theorem 1

The proof follows directly from Lemma H.1 in Chernozhukov et al. [2021]. It remains to verify the approximate ergodicity condition (E) and the estimation error condition (A) of Lemma H.1 in Chernozhukov et al. [2021] hold in the present setting with additional  $l_1$  regularization on the covariate space and treated observations across the whole units/time-space.

Let  $n = |\Pi|$  and  $\delta_{1n}, \delta_{2n}, \gamma_{1n}, \gamma_{2n}$  be sequences of numbers converging to 0.

- (E) With probability  $1 - \gamma_{1n}$  the randomization distribution  $\hat{F}(x) = \frac{1}{n} \sum_{\pi \in \Pi} \mathbf{1} \left\{ S \left( \hat{U}_\pi \right) < x \right\}$  is approximately ergodic for  $F(x) = P[S(u < x)]$ , namely  $\sup_{x \in \mathbb{R}} \left| \hat{F}(x) - F(x) \right| \leq \delta_{1n}$ .

(A) With probability  $1 - \gamma_{2n}$ , the estimation errors are small:

1. The mean squared error is small with  $n^{-1} \sum_{\pi \in \Pi} \left( S(\hat{U}_\pi) - S(U_\pi) \right)^2 \leq \delta_{2n}^2$ ;
2. The pointwise error at  $\pi = \text{Identity permutation}$  is small with  $\left| S(\hat{U}) - S(U) \right| \leq \delta_{2n}$ ;
3. The pdf of  $S(U)$  is bounded above by a constant D.

The following Lemmas B.1-B.4 verify the conditions (E) and (A), each for the iid permutations and the moving block permutations. Notice that condition (A.3) is already satisfied by Assumption 3.

**Lemma B.1** (Ergodicity condition (E) for iid permutations). *Suppose that Assumption 2.1 and 3 hold, and let  $\Pi$  be the set of all permutations. If  $|\mathcal{M}| < |\mathcal{O}|$ , then*

$$P \left[ \sup_{x \in \mathbb{R}} \left| \hat{F}(x) - F(x) \right| \leq \delta_{1n} \right] \geq 1 - \gamma_T,$$

where  $\gamma_T = \sqrt{\pi / (2 + 2 \lfloor |\mathcal{O}| / |\mathcal{M}| \rfloor)} / \delta_{1n}$

*Proof.* Recall that in the case of Assumption 2.1,  $\Pi$  is the set of all bijections  $\pi$  on  $\{1, \dots, T\}$ . Let  $b(x) : x \in \mathbb{R}^{|\mathcal{O}| \rightarrow \mathcal{O}}$  be any enumeration of the elements in  $\mathcal{O}$ . Let  $k_{\mathcal{M}} = \lfloor |\mathcal{O}| / |\mathcal{M}| \rfloor$  and define the set of indices

$$b_i = \begin{cases} \mathcal{M} & i = 0 \\ \{b((i-1) * |\mathcal{M}| + 1), \dots, b((i-1) * |\mathcal{M}| + |\mathcal{M}|)\} & i = 1, \dots, k_{\mathcal{M}}. \end{cases}$$

Since  $S(U)$  only depends on  $b_0$ , we can define

$$Q(x; U_{b_0}) = \mathbf{1}\{S(U_{b_0}) \leq x\} - F(x).$$

Therefore

$$\tilde{F}(x) - F(x) = |\Pi|^{-1} \sum_{\pi \in \Pi} Q(x; U_{\pi(b_0)}).$$

Because  $Q(x; u)$  only depends on the residuals in  $\mathcal{M}$ , the value of  $\sum_{\pi \in \Pi} Q(U_{\pi(b_i)})$  does not

depend on  $i$ . Hence, we can write

$$\begin{aligned}\tilde{F}(x) - F(x) &= |\Pi|^{-1} \sum_{\pi \in \Pi} Q(x; U_{\pi(b_0)}) \\ &= k_{\mathcal{M}}^{-1} \sum_{i=0}^{k_{\mathcal{M}}} \left( |\Pi|^{-1} \sum_{\pi \in \Pi} Q(x; U_{\pi(b_i)}) \right) \\ &= |\Pi|^{-1} \sum_{\pi \in \Pi} \left( k_{\mathcal{M}}^{-1} \sum_{i=0}^{k_{\mathcal{M}}} Q(x; U_{\pi(b_i)}) \right)\end{aligned}$$

By Jensen's inequality

$$\left[ \sup_{x \in \mathbb{R}} \left| \tilde{F}(x) - F(x) \right| \right] \leq |\Pi|^{-1} \sum_{\pi \in \Pi} E \left[ \sup_{x \in \mathbb{R}} \left| k_{\mathcal{M}}^{-1} \sum_{i=0}^{k_{\mathcal{M}}} Q(x; U_{\pi(b_i)}) \right| \right] \quad (\text{B.1})$$

We observe that for any  $\pi \in \Pi$

$$\begin{aligned}E \left[ \sup_{x \in \mathbb{R}} \left| k_{\mathcal{M}}^{-1} \sum_{i=0}^{k_{\mathcal{M}}} Q(x; U_{\pi(b_i)}) \right| \right] &= \int_0^1 P \left[ \sup_{x \in \mathbb{R}} \left| k_{\mathcal{M}}^{-1} \sum_{i=0}^{k_{\mathcal{M}}} Q(x; U_{\pi(b_i)}) \right| > z \right] dz \\ &\stackrel{(i)}{\leq} 2 \int_0^1 \exp(-2(k_{\mathcal{M}} + 1)z^2) dz \\ &< 2 \int_0^\infty \exp(-2(k_{\mathcal{M}} + 1)z^2) dz \\ &\stackrel{(ii)}{<} \sqrt{\pi/(2 + 2k_{\mathcal{M}})},\end{aligned} \quad (\text{B.2})$$

where (i) follows by the Dvoretzky-Kiefer-Wolfwitz inequality (e.g. Theorem 11.6 in Kosorok [2008]) and (ii) is a property of the normal distribution. Combining (B.1) and (B.2) yields

$$\left[ \sup_{x \in \mathbb{R}} \left| \tilde{F}(x) - F(x) \right| \right] \leq \sqrt{\pi/(2 + 2k_{\mathcal{M}})}.$$

The desired result in Lemma B.1 follows by the Markov's inequality.  $\square$

**Lemma B.2** (Ergodicity condition (E) for moving block permutations). *Suppose that Assumption 2.2 and 3 hold, and let  $\Pi$  be the set of all moving-block permutations. Assume  $|\mathcal{M}|_{\max} < T$ . Suppose that  $\forall i : \{u_{i,t}\}_{t=1}^T$  is stationary and strong mixing with  $\sum_{k=1}^\infty \alpha_{\text{mixing}}(k)$  is bounded by a constant  $M$ . Then there exists a constant  $c(M)$  such that for any  $\delta_{1n} > 0$*

$$P \left[ \sup_{x \in \mathbb{R}} \left| \hat{F}(x) - F(x) \right| \leq \delta_{1n} \right] \geq 1 - \gamma_T,$$

where  $\gamma_T = \left( c(M) \frac{\sqrt{|\mathcal{M}|_{\max} \log T}}{\sqrt{T}} \right) / \delta_{1n}$

*Proof.* For  $\pi \in \Pi$ , we define

$$s_t = \sum_{(i,t') \in \mathcal{M}} |U_{i,[t+t']_T}|$$

and

$$\check{F}(x) = |\Pi|^{-1} \sum_{1 \leq t \leq (T-1)} \mathbf{1}\{s_t \leq x\}.$$

It is straightforward to verify that  $\{S(U_\pi) : \pi \in \Pi\} = \{s_t : 1 \leq t \leq T\}$ . By Assumption 2.2,  $\{s_t\}$  is stationary for  $t \in \{1, \dots, T-1\}$  but not for  $t = T$  and the bounded pdf of  $s(U)$  implies the continuity of  $F(\cdot)$ . Let  $\tilde{\alpha}_{\text{mixing}}$  be the strong-mixing coefficients for  $\{s_t\}_{1 \leq t \leq T}$ . Then by Proposition 7.1 of Rio et al. [2017] it follows that

$$E \left[ \sup_{x \in \mathbb{R}} |\check{F}(x) - F(x)|^2 \right] \leq \frac{1}{|\Pi|} \left( 1 + 4 \sum_{k=0}^{|\Pi|-1} \tilde{\alpha}_{\text{mixing}}(k) \right) \left( 3 + \frac{\log |\Pi|}{2 \log 2} \right)^2.$$

Notice that  $\tilde{\alpha}_{\text{mixing}}(k) \leq |\mathcal{M}|_{\max} \alpha_{\text{mixing}}(k)$  and hence  $\sum_{k=0}^{|\Pi|-1} \tilde{\alpha}_{\text{mixing}}(k) \leq |\mathcal{M}| \cdot M$ . Since by Definition 2 the number of possible permutation is  $|\Pi| = T$ , it follows that

$$E \left[ \sup_{x \in \mathbb{R}} |\check{F}(x) - F(x)|^2 \right] \leq \frac{1}{T} (1 + 4 |\mathcal{M}|_{\max} \cdot M) \left( 3 + \frac{\log T}{2 \log 2} \right)^2.$$

By Liapunov's inequality

$$\begin{aligned} E \left[ \sup_{x \in \mathbb{R}} |\check{F}(x) - F(x)| \right] &\leq \sqrt{E \left[ \sup_{x \in \mathbb{R}} |\check{F}(x) - F(x)|^2 \right]} \\ &\leq \sqrt{\frac{1 + 4 |\mathcal{M}|_{\max} \cdot M}{T} \left( 3 + \frac{\log T}{2 \log 2} \right)} \end{aligned} \quad (\text{B.3})$$

Since  $T\check{F}(x) - (T-1)\check{F}(x) = \mathbf{1}\{s_0 \leq x\}$ , it follows that

$$\begin{aligned} \sup_{x \in \mathbb{R}} |\tilde{F}(x) - \check{F}(x)| &= \sup_{x \in \mathbb{R}} \left| \left( \frac{T-1}{T} \check{F}(x) + \frac{1}{T} \mathbf{1}\{s_0 \leq x\} \right) - \check{F}(x) \right| \\ &= \sup_{x \in \mathbb{R}} \left| \frac{1}{T} (\check{F}(x) + \mathbf{1}\{s_0 \leq x\}) - \check{F}(x) \right| \\ &\leq \frac{2}{T}, \end{aligned} \quad (\text{B.4})$$

as both terms,  $\check{F}(x)$  and  $\mathbf{1}\{s_0 \leq x\}$ , are bounded by 1. Combining (B.3) and (B.4), we obtain that

$$E \left[ \sup_{x \in \mathbb{R}} |\tilde{F}(x) - F(x)| \right] \leq \sqrt{\frac{1 + 4 |\mathcal{M}|_{\max} \cdot M}{T} \left( 3 + \frac{\log T}{2 \log 2} \right)} + \frac{2}{T}.$$

The desired result follows by Markov's inequality.  $\square$

**Lemma B.3** (Estimation error condition (A) for iid permutations). *Let  $\mathcal{M}$  be fixed. Assume that there exists a constant  $Q > 0$  such that  $\|S(U) - S(V)\| \leq Q \|\mathbf{W} \circ (U - V)\|_2$  for any  $U, V \in \mathbb{R}^{N \times T}$ . Suppose further that Assumption 4 holds, then conditions (A.1) and (A.2) are satisfied.*

*Proof.* For  $(i, t), (j, s) \in \{1, \dots, N\} \times \{1, \dots, T\}$ , we define  $A_{(i,t),(j,s)} = \{\pi \in \Pi : \pi(i, t) = (j, s)\}$ . Recall that under Assumption 2.1  $\Pi$  is the set of all bijections on  $\{1, \dots, N\} \times \{1, \dots, T\}$ . Thus,  $|A_{(i,t),(j,s)}| = (NT - 1)!$ . It follows that for any  $(i, t) \in \{1, \dots, N\} \times \{1, \dots, T\}$

$$\begin{aligned}
\sum_{\pi \in \Pi} \left( \hat{U}_{\pi(i,t)} - U_{\pi(i,t)} \right)^2 &= \sum_{(j,s)} \sum_{\pi \in A_{(i,t),(j,s)}} \left( \hat{U}_{\pi(i,t)} - U_{\pi(i,t)} \right)^2 \\
&= \sum_{(j,s)} \sum_{\pi \in A_{(i,t),(j,s)}} \left( \hat{U}_{(j,s)} - U_{(j,s)} \right)^2 \\
&= |A_{(i,t),(j,s)}| \sum_{(j,s)} \left( \hat{U}_{(j,s)} - U_{(j,s)} \right)^2 \\
&= (NT - 1)! \left\| \hat{U} - U \right\|_2^2
\end{aligned} \tag{B.5}$$

By assumption, we have

$$\begin{aligned}
\frac{1}{|\Pi|} \sum_{\pi \in \Pi} \left( S(\hat{U}_\pi) - S(U_\pi) \right)^2 &\leq \frac{Q}{|\Pi|} \sum_{\pi \in \Pi} \left\| \mathbf{W} \circ (\hat{U}_\pi - U_\pi) \right\|_2^2 \\
&\leq \frac{Q}{|\Pi|} \sum_{\pi \in \Pi} \sum_{(i,t) \in \mathcal{M}} \left( \hat{U}_{\pi(i,t)} - U_{\pi(i,t)} \right)^2 \\
&\leq \frac{Q}{|\Pi|} \sum_{(i,t) \in \mathcal{M}} \sum_{\pi \in \Pi} \left( \hat{U}_{\pi(i,t)} - U_{\pi(i,t)} \right)^2
\end{aligned}$$

Using  $|\Pi| = (NT)!$  and applying (B.5) it follows that

$$\begin{aligned}
\frac{1}{|\Pi|} \sum_{\pi \in \Pi} \left( S(\hat{U}_\pi) - S(U_\pi) \right)^2 &\leq \frac{Q}{(NT)!} \sum_{(i,t) \in \mathcal{M}} (NT - 1)! \left\| \hat{U} - U \right\|_2^2 \\
&\leq \frac{Q}{(NT)!} |\mathcal{M}| (NT - 1)! \left\| \hat{U} - U \right\|_2^2 \\
&\leq \frac{Q |\mathcal{M}|}{NT} \left\| \hat{U} - U \right\|_2^2
\end{aligned}$$

Since  $|\mathcal{M}|$  is fixed, condition (A.1) holds by Assumption 4.1.

Recall that  $S(U)$  only depends on the elements of  $U$  in the set  $\mathcal{M}$ . Let  $U_{\mathcal{M}} = \{U_{it} : (i, t) \in \mathcal{M}\}$ . The Lipschitz property of  $S(\cdot)$  implies that

$$\begin{aligned} \left| S(\hat{U}) - S(U) \right| &= \left| S(\hat{U}_{\mathcal{M}}) - S(U_{\mathcal{M}}) \right| \\ &\leq k \left| \hat{U}_{\mathcal{M}} - U_{\mathcal{M}} \right| \end{aligned}$$

Condition (A.2) follows by Assumption 4.2. The proof is complete.  $\square$

**Lemma B.4** (Estimation error condition (E) for moving block permutations). *Let  $\mathcal{M}$  be fixed and suppose  $|\mathcal{M}|_{\max} < T$ . Assume that there exists a constant  $Q > 0$  such that  $\|S(U) - S(V)\| \leq Q \|\mathbf{W} \circ (U - V)\|_2$  for any  $U, V \in \mathbb{R}^{N \times T}$ . Suppose further that Assumption 4 holds, then conditions (A.1) and (A.2) are satisfied.*

*Proof.* Notice that for moving block permutations

$$\sum_{(i,t) \in \mathcal{M}} \sum_{\pi \in \Pi} \left( \hat{U}_{i,\pi(t)} - U_{i,\pi(t)} \right)^2 \leq |\mathcal{M}|_{\max} \left\| \hat{U} - U \right\|_2^2, \quad (\text{B.6})$$

since the permutations shift the residuals once over the full time interval.

By assumption, we have

$$\begin{aligned} \frac{1}{|\Pi|} \sum_{\pi \in \Pi} \left( S(\hat{U}_{\pi}) - S(U_{\pi}) \right)^2 &\leq \frac{Q}{|\Pi|} \sum_{\pi \in \Pi} \left\| \mathbf{W} \circ (\hat{U}_{\pi} - U_{\pi}) \right\|_2^2 \\ &\leq \frac{Q}{|\Pi|} \sum_{\pi \in \Pi} \sum_{(i,t) \in \mathcal{M}} \left( \hat{U}_{i,\pi(t)} - U_{i,\pi(t)} \right)^2 \\ &\leq \frac{Q}{|\Pi|} \sum_{(i,t) \in \mathcal{M}} \sum_{\pi \in \Pi} \left( \hat{U}_{i,\pi(t)} - U_{i,\pi(t)} \right)^2 \end{aligned} \quad (\text{B.7})$$

$$(\text{B.8})$$

Using  $|\Pi| = T$  and applying (B.6) it follows that

$$\frac{1}{|\Pi|} \sum_{\pi \in \Pi} \left( S(\hat{U}_{\pi}) - S(U_{\pi}) \right)^2 \leq \frac{Q}{T} |\mathcal{M}|_{\max} \left\| \hat{U} - U \right\|_2^2$$

Since  $|\mathcal{M}|$  is fixed and  $|\mathcal{M}|_{\max} < T$ , condition (A.1) holds by Assumption 4.1.

Recall that  $S(U)$  only depends on the elements of  $U$  in the set  $\mathcal{M}$ . Let  $U_{\mathcal{M}} = \{U_{it} :$

$(i, t) \in \mathcal{M}$ . The Lipschitz property of  $S(\cdot)$  implies that

$$\begin{aligned} \left| S(\hat{U}) - S(U) \right| &= \left| S(\hat{U}_{\mathcal{M}}) - S(U_{\mathcal{M}}) \right| \\ &\leq k \left| \hat{U}_{\mathcal{M}} - U_{\mathcal{M}} \right| \end{aligned}$$

Condition (A.2) follows by Assumption 4.2. The proof is complete.  $\square$

### B.3 Proof of Lemma 1

Assume that

(L1.1) Assumption 1 holds,

(L1.2)  $\|\mathbf{L}\|_* \leq \Lambda_L, \|\mathbf{H}\|_{1,e} \leq \Lambda_H, \|\beta\|_{1,e} \leq \Lambda_\beta,$

(L1.3)  $\exists \kappa_1 : \max_{1 \leq j \leq N} T^{-1} \sum_{t=1}^T E \left[ |u_{it}|^{2\kappa_1} \mid \mathcal{Z} \right] = O_P(1),$

(L1.4)  $\left\| N^{-1} \sum_{i=1}^N E \left[ U_i U_i^\top \mid \mathcal{Z} \right] \right\| = O_P(1),$

there exists a sequence  $\nu_{N,T} \geq 0$  such that

(L1.5)  $\nu_{N,T} (NT)^{-1} \left( \Lambda_L \sqrt{N \vee (N^{1/\kappa_1} T \log(N))} + PQ\Lambda_H c_H + J\Lambda_\beta c_\beta \right) = o(1)$

(L1.6)  $(NT)^{-1} \sum_{i=1}^N \sum_{t=1}^T (\hat{\mathbf{Y}}_{it}^{0,\varepsilon} - \mathbf{Y}_{it}^{0,\varepsilon})^2 \leq \nu_{N,T} (NT)^{-1} \sum_{i=1}^N \sum_{t=1}^T (\hat{\mathbf{Y}}_{it}^{0,\varepsilon} - \mathbf{Y}_{it}^{0,\varepsilon})^2$

(L1.7)  $\forall_{(j,s) \in \mathcal{M}} : \left| \hat{\mathbf{Y}}_{js}^{0,\varepsilon} - \mathbf{Y}_{js}^{0,\varepsilon} \right| \leq \nu_{N,T} (NT)^{-1} \sum_{i=1}^N \sum_{t=1}^T (\hat{\mathbf{Y}}_{it}^{0,\varepsilon} - \mathbf{Y}_{it}^{0,\varepsilon})^2$

Define  $\Xi := \hat{\mathbf{Y}}^{0,\varepsilon} - \mathbf{Y}^{0,\varepsilon}$  and  $Q_{it} \in \mathbb{R}^{N \times T} : [Q_{it}]_{js} = \mathbf{1}\{(j, s) = (i, t)\}$ , i.e. the matrix of zeros except for the  $(i, t)$  element is 1. We thus can rewrite the model as

$$\mathbf{Y}_{it}(0) = \text{trace}(\mathbf{Q}_{it}^\top \mathbf{Y}^{0,\varepsilon}) + \mathbf{U}_{it} \tag{B.9}$$

Note that by definition the estimator (6) satisfies

$$\sum_{i=1}^N \sum_{t=1}^T \left( \mathbf{Y}_{it}(0) - \text{trace}(\mathbf{Q}_{it}^\top \hat{\mathbf{Y}}^{0,\varepsilon}) \right)^2 \leq \sum_{i=1}^N \sum_{t=1}^T \left( \mathbf{Y}_{it}(0) - \text{trace}(\mathbf{Q}_{it}^\top \mathbf{Y}^{0,\varepsilon}) \right)^2.$$

We plug-in (B.9) and reformulate to obtain

$$\begin{aligned}
\sum_{i=1}^N \sum_{t=1}^T \left( \text{trace}(\mathbf{Q}_{it}^\top \mathbf{Y}^{0,\varepsilon}) + \mathbf{U}_{it} - \text{trace}(\mathbf{Q}_{it}^\top \hat{\mathbf{Y}}^{0,\varepsilon}) \right)^2 &\leq \sum_{i=1}^N \sum_{t=1}^T (\mathbf{U}_{it})^2 \\
\sum_{i=1}^N \sum_{t=1}^T (\mathbf{U}_{it} - \text{trace}(\mathbf{Q}_{it}^\top \Xi))^2 &\leq \sum_{i=1}^N \sum_{t=1}^T (\mathbf{U}_{it})^2 \\
\sum_{i=1}^N \sum_{t=1}^T (\text{trace}(\mathbf{Q}_{it}^\top \Xi))^2 &\leq 2 \sum_{i=1}^N \sum_{t=1}^T \mathbf{U}_{it} \text{trace}(\mathbf{Q}_{it}^\top \Xi) \\
\sum_{i=1}^N \sum_{t=1}^T (\text{trace}(\mathbf{Q}_{it}^\top \Xi))^2 &\leq 2 \text{trace} \left( \left[ \sum_{i=1}^N \sum_{t=1}^T \mathbf{U}_{it} \mathbf{Q}_{it} \right]^\top \Xi \right) \\
\sum_{i=1}^N \sum_{t=1}^T (\text{trace}(\mathbf{Q}_{it}^\top \Xi))^2 &\leq 2 \text{trace}(\mathbf{U}^\top \Xi) \tag{B.10}
\end{aligned}$$

Usign  $\Xi = (\hat{\mathbf{L}} - \mathbf{L}) + \left[ \overline{\mathbf{XZ}}_{it}(\hat{H} - \bar{H}) \right]_{it} + \left[ \mathbf{v}_{it}^\top(\hat{\beta} - \beta) \right]_{it}$  and applying Lemma B.5, it follows that

$$\begin{aligned}
\text{trace}(\mathbf{U}^\top \Xi) &= \text{trace}(\mathbf{U}^\top (\hat{\mathbf{L}} - \mathbf{L})) + \text{trace}(\mathbf{U}^\top \left[ \overline{\mathbf{XZ}}_{it}(\hat{H} - \bar{H}) \right]_{it}) + \text{trace}(\mathbf{U}^\top \left[ \mathbf{v}_{it}^\top(\hat{\beta} - \beta) \right]_{it}) \\
&\stackrel{(i)}{\leq} \|u\| \cdot \left\| \hat{\mathbf{L}} - \mathbf{L} \right\|_* + 2PQ\Lambda_H \delta_H + 2J\Lambda_\beta \delta_\beta \\
&\leq 2(\lambda_L \|u\| + PQ\Lambda_H \delta_H + J\Lambda_\beta \delta_\beta) \tag{B.11}
\end{aligned}$$

where the first term in (i) follows from the trace duality property. To bound  $\|u\|$ , we apply Lemma H.10 of Chernozhukov et al. [2021] and get

$$\begin{aligned}
\sum_{i=1}^N \sum_{t=1}^T (\text{trace}(\mathbf{Q}_{it}^\top \Xi))^2 &\leq 4(\lambda_L \|u\| + PQ\Lambda_H \delta_H + J\Lambda_\beta \delta_\beta) \\
\sum_{i=1}^N \sum_{t=1}^T (\text{trace}(\mathbf{Q}_{it}^\top \Xi))^2 &= O \left( \Lambda_L \sqrt{N \vee (N^{1/\kappa_1} T \log(N))} + PQ\Lambda_H c_H + J\Lambda_\beta c_\beta \right) \\
(NT)^{-1} \sum_{i=1}^N \sum_{t=1}^T (\text{trace}(\mathbf{Q}_{it}^\top \Xi))^2 &= O \left( (NT)^{-1} \right. \\
&\quad \left. \left( \Lambda_L \sqrt{N \vee (N^{1/\kappa_1} T \log(N))} + PQ\Lambda_H c_H + J\Lambda_\beta c_\beta \right) \right) \tag{B.12}
\end{aligned}$$

The first result in Lemma 1 follows from applying Assumptions (L1.5) and (L1.6) to (B.12), the second result by applying Assumptions (L1.5) and (L1.7).



**Lemma B.5.** Assume that there exist two constants  $\delta_H, \delta_\beta$  such that  $\max_{1 \leq h \leq PQ} \sum_{i=1}^N \sum_{t=1}^T u_{it} \overline{\mathbf{XZ}}_{it,h} \leq \delta_H$  and  $\max_{1 \leq b \leq J} \sum_{i=1}^N \sum_{t=1}^T u_{it} V_{it,b} \leq \delta_H$ . Then it holds that  $\text{trace} \left( \mathbf{U}^\top \left[ \overline{\mathbf{XZ}}_{it} (\hat{H} - \bar{H}) \right]_{it} \right) \leq 2PQ\delta_H\Lambda_H$  and  $\text{trace} \left( \mathbf{U}^\top \left[ V_{it} (\hat{\beta} - \beta) \right]_{it} \right) \leq 2J\delta_\beta\Lambda_\beta$

*Proof.* Recall that  $\sum_{h=1}^{PQ} \bar{H}_h \leq \Lambda_H$ . Thus

$$\begin{aligned} \text{trace} \left( \mathbf{U}^\top \left[ \overline{\mathbf{XZ}}_{it} (\hat{H} - \bar{H}) \right]_{it} \right) &= \sum_{i=1}^N \sum_{t=1}^T \sum_{h=1}^{PQ} \varepsilon_{it} \overline{\mathbf{XZ}}_{it,h} (\hat{H}_h - \bar{H}_h) \\ &= \sum_{h=1}^{PQ} (\hat{H}_h - \bar{H}_h) \sum_{i=1}^N \sum_{t=1}^T \varepsilon_{it} \overline{\mathbf{XZ}}_{it,h} \\ &\leq \delta_H \sum_{h=1}^{PQ} (\hat{H}_h - \bar{H}_h) \\ &\leq 2PQ\delta_H\Lambda_H. \end{aligned}$$

The proof of  $\text{trace} \left( \mathbf{U}^\top \left[ V_{it} (\hat{\beta} - \beta) \right]_{it} \right) \leq 2J\delta_\beta\Lambda_\beta$  is equivalent.  $\square$

## C Formulation of data generating process

The data-generating process is defined by the following equations:

$$\mathbf{Y} = \tau \mathbf{W} + \mathbf{L} + \mathbf{XHZ} + [\mathbf{V}_{it}^\top \boldsymbol{\beta}]_{it} + \boldsymbol{\Gamma} \mathbf{1}_T^\top + \mathbf{1}_N (\boldsymbol{\Delta})^\top + \mathbf{U}, \quad \mathbf{Y} \in \mathbb{R}^{N \times T}$$

$$\mathbf{W}_{it} \sim \text{Bernoulli}(w)$$

$$\mathbf{L} = \mathbf{U} (\sigma \cdot \mathbf{1}) \mathbf{V}^\top, \quad \sigma_j = \begin{cases} \sim \exp(\zeta_L), & j \leq \text{rank}_L \\ 0 & j > \text{rank}_L \end{cases}, \quad (\mathbf{U}, \Sigma, \mathbf{V}^\top) = \text{svd}(\mathbf{L}'), \quad [\mathbf{L}']_{it} \sim \mathcal{N}(0, 1)$$

$$\mathbf{X} = [\eta_1 \mathbf{X}_1, \dots, \eta_N \mathbf{X}_N]^\top \in \mathbb{R}^{N \times p}, \quad \mathbf{X}_i \sim (\mathbf{0}, \boldsymbol{\Sigma}_X), \quad [\boldsymbol{\Sigma}_X]_{ab} = \begin{cases} 1, & a=b \\ \sim \mathcal{U}(0, \sigma_{\max}), & a \neq b \end{cases}, \quad \eta_i \sim \mathcal{U}(0, 1)$$

$$\mathbf{H}_{it} = \eta_{it} \zeta_{it}, \quad \eta_{it} \sim \mathcal{N}(0, h_{\text{size}}), \quad \zeta_{it} \sim \text{Bernoulli}(h_{\text{prob}})$$

$$\mathbf{Z} = [\eta_1 \mathbf{Z}_1, \dots, \eta_T \mathbf{Z}_T] \in \mathbb{R}^{p \times T}, \quad \mathbf{Z}_t \sim (\mathbf{0}, \boldsymbol{\Sigma}_Z), \quad [\boldsymbol{\Sigma}_Z]_{ab} = \begin{cases} 1, & a=b \\ \sim \mathcal{U}(0, \sigma_{\max}), & a \neq b \end{cases}, \quad \eta_t \sim \mathcal{U}(0, 1)$$

$$\mathbf{V}_{it} \sim (\mathbf{0}, \mathbf{1}), \quad \mathbf{V}_{it} \in \mathbb{R}^B$$

$$\boldsymbol{\beta}_b = \eta_b \zeta_b, \quad \eta_b \sim \mathcal{N}(0, b_{\text{size}}), \quad \zeta_b \sim \text{Bernoulli}(b_{\text{prob}})$$

$$\boldsymbol{\Gamma}_i \sim \mathcal{N}(0, 1)$$

$$\boldsymbol{\Delta}_t \sim \mathcal{N}(0, 1)$$

$$\mathbf{U}_{it} \sim \mathcal{N}(0, \sigma_{\text{eps}})$$

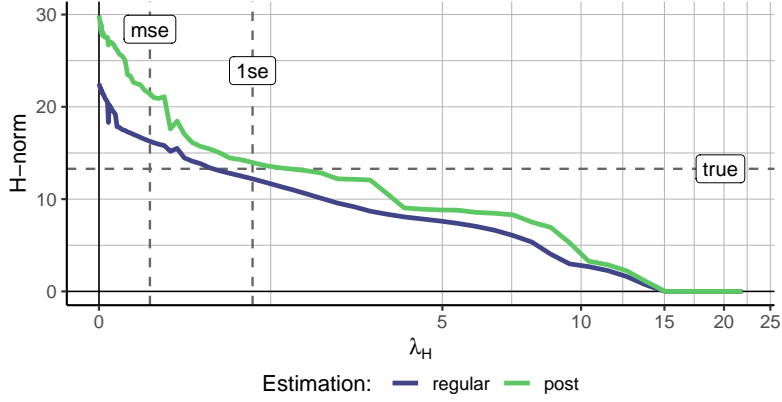
If not specified otherwise, the following parameters for the data-generating process are used:  $N = 100$ ,  $T = 80$ ,  $\tau = 1$ ,  $\text{rank}_L = 5$ ,  $w = 0.1$ ,  $\sigma_{\max} = 0.8$ ,  $p = 50$ ,  $q = 20$ ,  $h_{\text{size}} = 1$ ,  $h_{\text{prob}} = 0.025$ ,  $B = 1000$ ,  $b_{\text{size}} = 1$ ,  $b_{\text{prob}} = 0.02$ ,  $\sigma_{\text{eps}} = 1$ . The number of folds for the cross-validation is set to 5. To ensure comparability across individual simulation runs, the Bernoulli-distributed random variables can be replaced by draws without replacement and respective ratios for small sample sizes.

## D Additional simulation results for H (ASR-H)

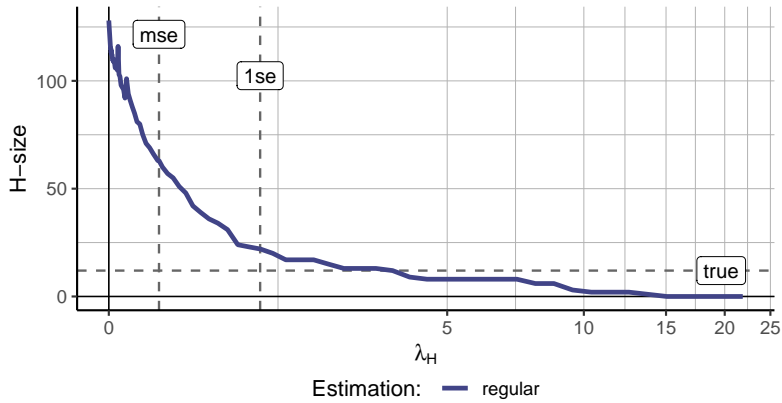
### D.1 ASR-H: Choice of optimal penalty parameter

Figure 6 displays the aggregate level on all coefficients for different values of  $\lambda_H$ : 6a shows the element-wise  $l_1$  norm of the estimated matrix  $\hat{\mathbf{H}}$  and 6b the number of non-zero coefficients. Both aggregation measures coincide with the observed pattern in Figure 1. The number of coefficients in the constituted model by specific values of the penalty parameter decreases very fast already for low levels of regularization. In accordance with Figure 1, the first coefficients to be eliminated are the ones with a small dedicated parameter estimate, letting the norm of the coefficients decline slower than the number of non-zero coefficients. The last coefficients to be regularized out are the ones with the highest absolute coefficient estimate.

Figure 6 further illustrates that the *post*-regularization estimation without the penalty terms in the estimation equation (6) and including only the covariates from the selected model by the *regular* matrix completion estimation yields larger coefficient estimates in absolute terms as they are not shrunk by regularization. The values for the post-estimation are not shown in Figure 6b as its model coincides with the regular estimation by construction.



(a) Element-wise  $l_1$  norm of  $\hat{\mathbf{H}}$



(b) Number of non-zero elements in  $\hat{\mathbf{H}}$

Figure 6: Element-wise  $l_1$  norm (a) and number of non-zero elements (b) of  $\hat{\mathbf{H}}$  estimate for different values of regularization parameter  $\lambda_H$

Note: 'mse' and '1se' show determined  $\lambda_H$  based on  $mse$  and  $1se$  optimality criteria, 'true' denotes the true value in the data. The number of non-zero elements is equal for regular and post-regularization estimation

## D.2 ASR-H: Accuracy of treatment effect estimates by signal-to-noise ratio

Figure 7 shows the estimated treatment effects on the treated for different signal-to-noise ratios. With the true parameters for all explanatory covariates and the fixed treatment effect  $\tau$  set to 1, the signal-to-noise ratio is given by the inverse of the error-term standard deviation  $\sigma_\epsilon$ . All versions of the matrix completion estimator exhibit increasing variance with decreasing signal strength. This is as expected as with larger random shocks, it is

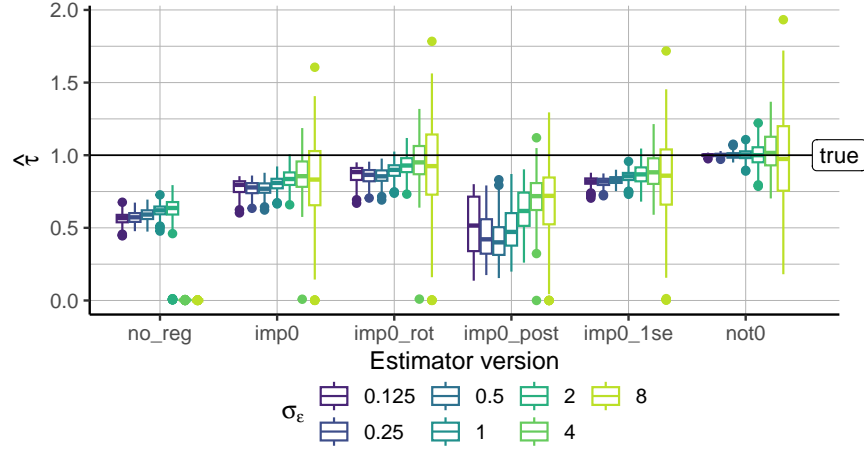


Figure 7: Boxplot of  $\hat{\tau}$  by estimation method.

Note: Signal-to-noise ratio is given by  $1/\sigma_\epsilon$ .  $N = 100$ ,  $T = 80$ . 1400 runs per signal-to-noise ratio.

more difficult for the estimator to filter out the random components and identify the true signals. The bias pattern of the estimators with the imposed null hypothesis is equivalent to the insights from Section 4.3. The regularization without imposing the null hypothesis consistently outperforms all other estimators. Among the version with imposed null, the rule-of-thumb correct remains the best-performing estimator, in particular for small signal strengths.

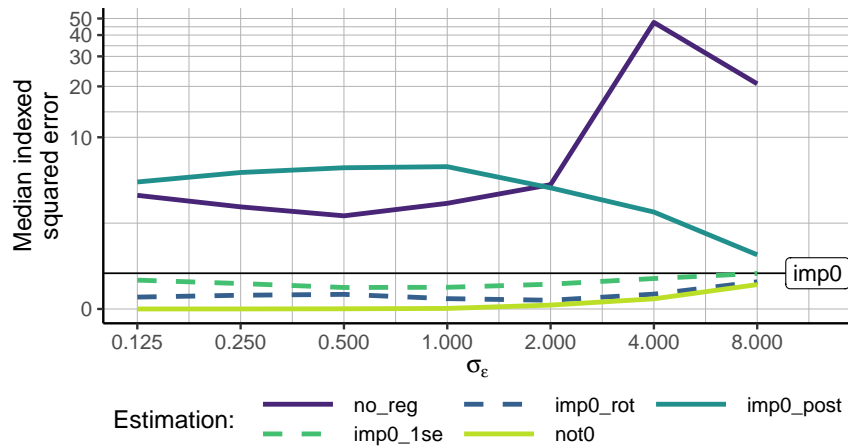


Figure 8: Median indexed squared error of  $\hat{\tau}$  by estimation method.

Note: *Indexed* measures are divided by the estimate of the *imp0* model. Signal-to-noise ratio is given by  $1/\sigma_\epsilon$ .  $N = 100$ ,  $T = 80$ . 1400 runs per signal-to-noise ratio. Transformed y-axis.

In Figure 8, we illustrate the median indexed squared error by the non-regularized esti-

mates, equivalent as described in Section 4.3. For weak signals, the unregularized estimator heavily struggles to extract the true parameters for its high-dimensional model. All regularized estimator versions perform clearly better as they restrict the focus to a few covariate parameters only. It is worth noting that the differences in accuracy for the estimators with regularization vanish with a decreasing signal-to-noise ratio.

### D.3 ASR-H: MSE of coefficient estimates in H

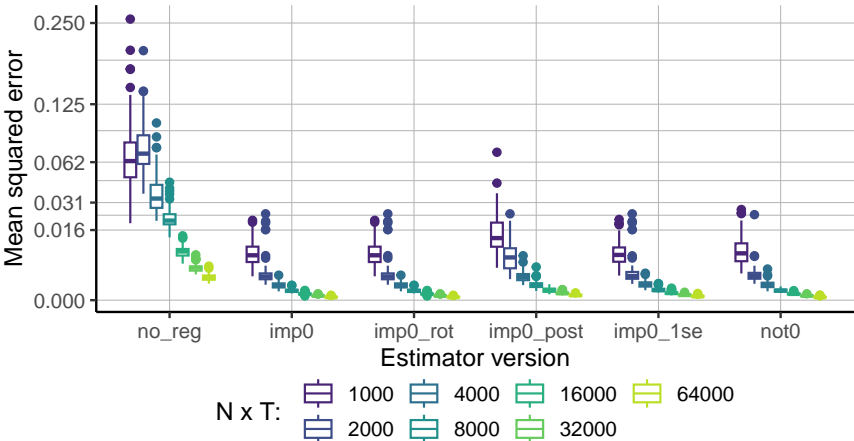


Figure 9: Mean squared error of  $\mathbf{H}$ -coefficients. Note:  $N = 100$ ,  $T \in \{10, 20, 40, 80, 160, 320, 640\}$ . 700 simulations per sample size. Transformed y-axis.

In Figure 9, a boxplot representation illustrates the mean squared errors associated with the estimated coefficients across multiple simulation runs. Notably, both the magnitude and variance of coefficient estimation errors exhibit a pronounced decline as the sample size increases. It is observed that post-regularization estimates exhibit the highest MSE among all versions of the estimator considered. Figure 9 shows the boxplot of the mean squared errors of the estimated coefficients for each simulation run. The magnitude and the variance of the coefficient estimation errors are rapidly decreasing in the sample size. The post-regularization estimates exhibit the largest mse among all estimator versions. In light of the fact that the second stage produces unbiased estimates through the exclusion of

$l_1$ -regularization, it follows that the post-regularization coefficient estimates are susceptible to increased variability.

#### D.4 ASR-H: Model selection property for different signal-to-noise ratios

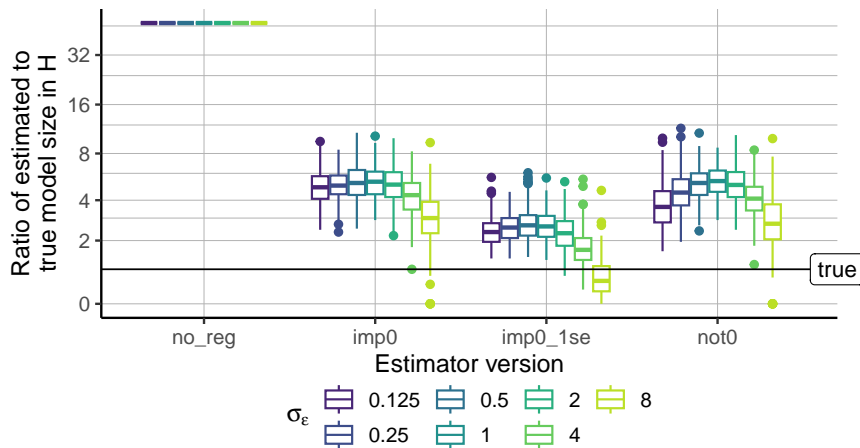
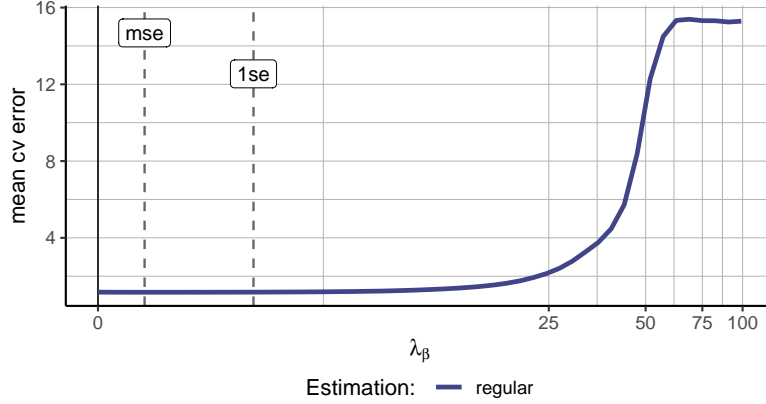


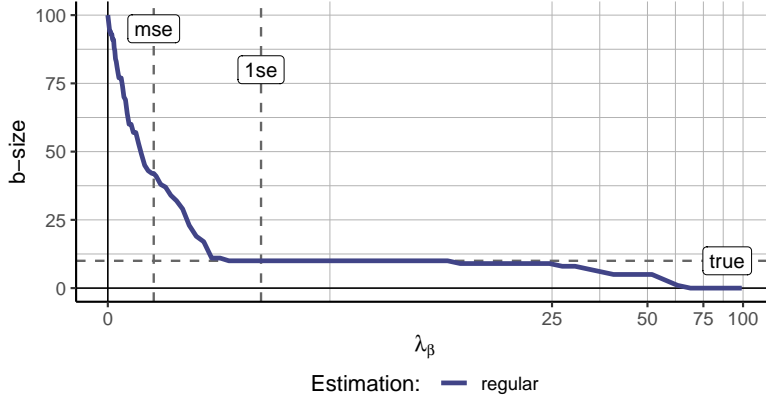
Figure 10: Ratio between the estimated and true model size in  $\mathbf{H}$ .

Note: Signal-to-noise ratio is given by  $1/\sigma_\epsilon$ . 1400 simulations per signal strength.  $N = 100$ ,  $T = 80$ . The number of non-zero elements is equal for regular, rule-of-thumb correction, and post-regularization estimation. Transformed y-axis.

Figure 10 illustrates that the determined model size remains stable when the signal possesses considerable strength. However, for signal-to-noise ratios approaching very small magnitudes, all estimators tend to discern fewer informative parameters within the model. Consequently, this discernment results in estimated models that are even sparser than the true model.



(a) Mean error of out-of-sample prediction over cross-validation folds of  $\beta$  for different values of regularization parameter  $\lambda_\beta$



(b) Number of non-zero elements in  $\beta$  for different values of regularization parameter  $\lambda_\beta$ . The number of non-zero elements is equal for regular and post-regularization estimation

Figure 11: Choice of  $\beta$  by cross-validation

Note: 'mse' and '1se' show determined  $\lambda_\beta$  based on *mse* and *1se* optimality criteria. 'true' denotes the true value in the data.

## E Additional simulation results for $\hat{\beta}$ (ASR- $\hat{\beta}$ )

### E.1 ASR- $\hat{\beta}$ : Choice of optimal penalty parameters by cross-validation

Figure 11 presents the outcomes of the cross-validation-based determination of the penalization parameter  $\beta$ . The inherent convexity of the optimization problem is evident in Figure 11b, facilitating efficient numerical evaluation. The findings indicate that the utilization of cross-validation samples tends toward conservatism [Hastie et al., 2009]. Notably, the *1se*

criterion opts for a notably diminished model size while maintaining proximity to the optimal value of the objective function. The empirical findings illustrated in Figure 11b underscore that the model size determined by the *lse* criterion aligns closely with the true number of non-zero parameters. In contrast, the penalization using the *mse* optimality criterion appears to not shrink the model strongly enough.

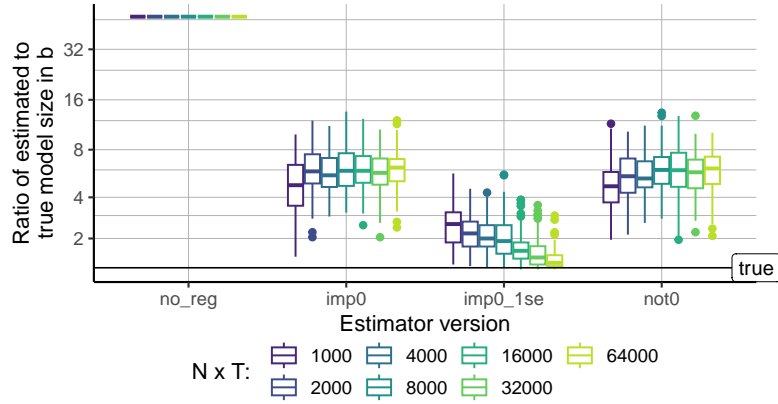
## E.2 ASR- $\hat{\beta}$ : Model selection property

We compare the dimensions of the obtained model, given by the count of non-zero coefficients in the  $\beta$ , to the true size of the generated sample in order to evaluate the ability of the proposed estimator in model selection. Note that neither the post-regularization nor the rule-of-thumb correction estimates alter the model size and, accordingly, are omitted in the following results.

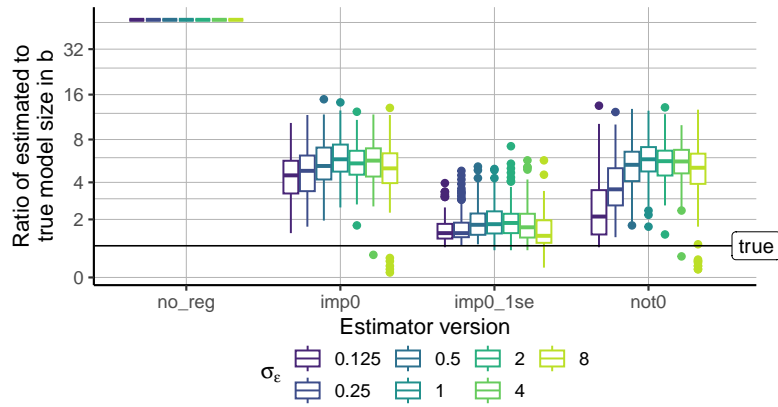
Figure 12a illustrates a pronounced reduction in the count of non-zero coefficients within the vector  $\beta$  when employing a regularized estimator. The baseline *mse* optimal cross-validation yields a model that exceeds the true size by approximately sixfold. Contrastingly, employing the *lse* criterion in cross-validation effectively contracts the non-zero coefficients in  $\beta$ , aligning them closely with the correct model size. Notably, with an expanding sample size, the *lse* estimator adeptly exploits the available data, leading to a convergence of the determined model size towards its true value.

Figure 12b delineates that the ascertained model size exhibits resilience as soon as the signal reaches minimal strengths. Nevertheless, as the signal-to-noise ratio is at a very small magnitude, all estimators tend towards discerning fewer parameters as informative. This propensity leads to the determination of a sparser model that aligns more closely with the true model size. However, it is important to underscore that this observed trend is unlikely to stem from enhanced model selection capabilities. Rather, it is probable that in scenarios characterized by weak signal strengths, the task of pinpointing a relevant parameter becomes inherently more challenging.





(a) Ratio between the estimated and true model size in  $\mathbf{H}$ .  
 Note:  $N = 100$ ,  $T \in \{10, 20, 40, 80, 160, 320, 640\}$ . 700 simulations per sample size. The number of non-zero elements is equal for regular, rule-of-thumb correction, and post-regularization estimation. Transformed y-axis.



(b) Ratio between the estimated and true model size in  $\mathbf{H}$ .  
 Note: Signal-to-noise ratio is given by  $1/\sigma_\epsilon$ . 1400 simulations per signal strength.  $N = 100$ ,  $T = 80$ . The number of non-zero elements is equal for regular, rule-of-thumb correction, and post-regularization estimation. Transformed y-axis.

Figure 12: Ratio between the estimated and true model size in  $\beta$  for different (a) sample size and (b) signal strength.